A competitive binding assay for RNA ligand discovery

Wintermans, S.E.L.

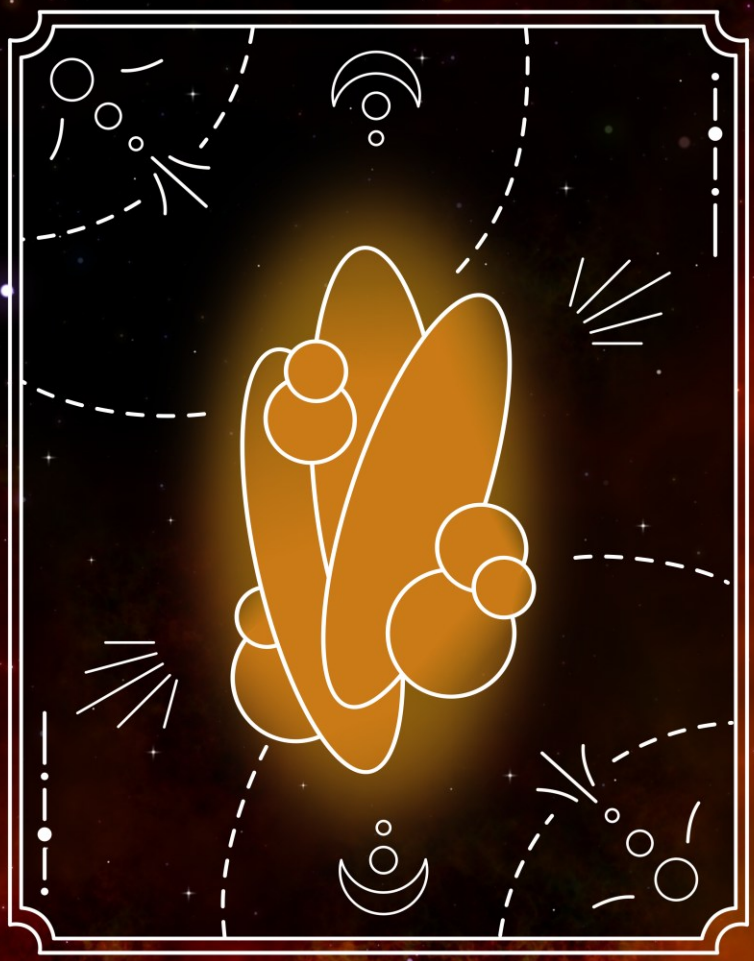

THE BACTERIA

Chapter 2

Development of a Competitive Binding ASsay for the $PreQ_1$ riboswitch

Parts of this chapter have been published in:

S.E.L. Wintermans, J.S. Hoffmann, V. van Kuijk, Y. Durmus, M.D. Tacoma, I. Broekhuizen, A.P.A. Janssen, H. van den Elst, B.R. van Doodewaerd, P.P. Geurink, M.E. Artola, R.C.L. Olsthoorn: *High-Throughput Competitive Binding Assay for Targeting RNA Tertiary Structures with Small Molecules: Application to Pseudoknots and G-Quadruplexes*. Nucleic Acids Research, (2025), *53* (16).

Introduction

Growing antibiotic-resistance is a massive global burden for public health which desperately calls for the development of new antimicrobials and novel therapeutic modalities. In drug development, it is common to target proteins that are essential to the lifecycle of pathogens, thereby killing bacteria (bactericidal compounds) or inhibiting their growth (bacteriostatic agents). However, the number of targetable proteins of a pathogen is limited, since not all proteins are implicated in essential processes and some proteins are difficult to target due to the lack of distinct or unique binding pockets[1–3]. Therefore, expanding the list of potential druggable targets by including RNA provides new therapeutic opportunities, which will be paramount in the fight against antibiotic resistant bacterial strains[4].

Riboswitches are promising and recently discovered RNA targets in bacteria[5]. These RNA structures are often found in the 5′-untranslated region (5′-UTR) of bacterial messenger RNA (mRNA) and can change conformation upon binding of a ligand, which ultimately leads to a change in gene expression[6–9]. As of yet, more than 55 different classes of riboswitches have been discovered and validated[10], and several of these have been described as antimicrobial drug targets. One such potential antibacterial target is the $PreQ_1$ riboswitch, which is involved in the biosynthesis of the hypermodified queuosine (Q) nucleoside (**Figure 2.1A**). Q occupies the anticodon wobble position of several tRNAs ($tRNA^{Tyr}$, $tRNA^{Asp}$, $tRNA^{His}$ and $tRNA^{Asn}$)[11,12] and plays an important role in the correct decoding of mRNA[13,14]. In particular, Q is important for viability and virulence of various bacteria[13,15,16].

The $PreQ_1$ riboswitch is known to directly regulate the expression of six proteins: four enzymes (QueCDEF) involved in the biosynthesis of $PreQ_1$ (a key precursor of Q) and two $PreQ_1$ transporter proteins (QueT and YhhQ)[17–20]. By binding to $PreQ_1$, the riboswitch either prematurely stops transcription by formation of a terminator hairpin (**Figure 2.1B**), or prevents translation by sequestering the Shine-Dalgarno (SD) sequence, a.k.a. the bacterial ribosome binding site (**Figure 2.1C**)[21,22]. Three classes of $PreQ_1$ riboswitches can be distinguished ($PreQ_1$-I, II and III), each with distinct structures and functions. This research focuses on the $PreQ_1$-I riboswitch, which is the smallest riboswitch known to date and is present in several clinically relevant human pathogenic bacteria, and therefore may be a suitable target for the discovery of new antibacterial drugs[23,17,21,24,25].

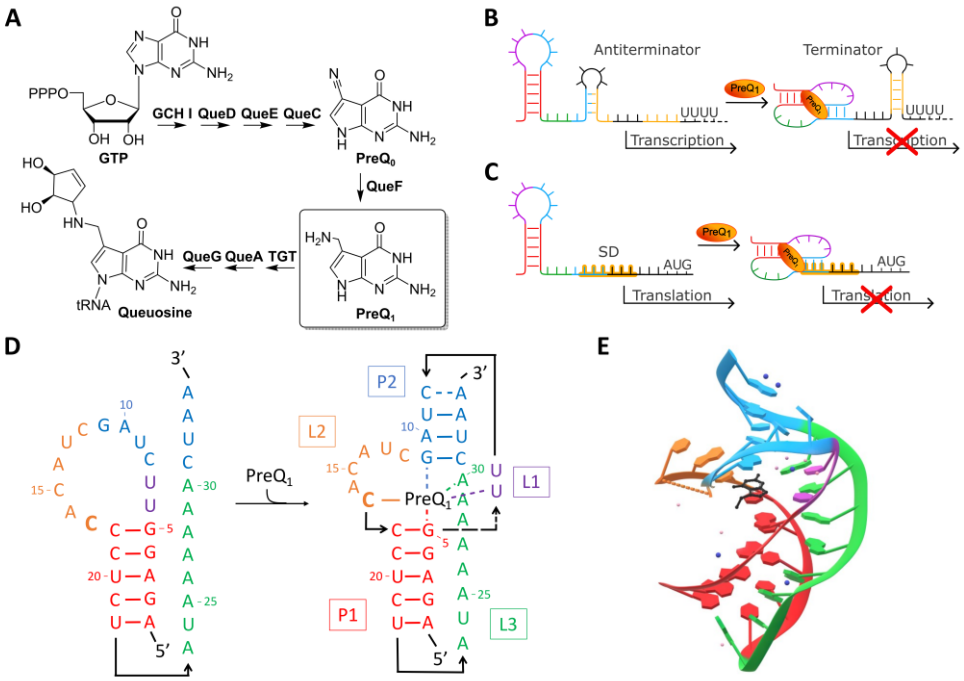

Figure 2.1. A) Biosynthetic pathway of Queuosine from GTP: enzymes involved and chemical structures of key intermediates $PreQ_0$ and $PreQ_1$ are shown. **B)** $PreQ_1$ riboswitch gene regulation: termination of transcription. Binding of $PreQ_1$ to the riboswitch leads to the formation of a terminator hairpin, thereby prematurely terminating transcription. **C)** $PreQ_1$ riboswitch gene regulation: prevention of translation. Binding of $PreQ_1$ to the riboswitch leads to the sequestration of the Shine-Dalgarno (SD) sequence, thereby preventing ribosomes from binding the mRNA and blocking translation. **D)** 2D structure of the *Bacillus subtilis* (*Bsu*) $PreQ_1$-I riboswitch in metabolite-free (left) or metabolite-bound (right) conformation. Interactions of $PreQ_1$ with several bases of the riboswitch are shown as dotted lines. **E)** 3D structure of the *Bsu* $PreQ_1$-I riboswitch bound to $PreQ_1$ (PBD: 3FU2).

When bound to $PreQ_1$, the $PreQ_1$-I riboswitch forms a hairpin (H)-type pseudoknot (PK) (**Figure 2.1D and 2.1E**)[26–28]. Stems P1 and P2 are connected by single-stranded loops (L1, L2 and L3) that can form tertiary interactions such as base triples with base pairs in the stem or interact with ligands to further stabilize the PK. $PreQ_1$-I pseudoknots have an unusually long L2 of 6 nucleotides, although intercalation of a $PreQ_1$ molecule at the interhelical junction supports efficient coaxial stacking[27]. $PreQ_1$ aptamers are able to bind $PreQ_1$ with nanomolar affinities and are able to distinguish between closely related purines, as demonstrated by Roth *et al.* for several $PreQ_1$ analogues binding to the *Bacillus subtilis* (*Bsu*) aptamer[17,29,30]. Tight $PreQ_1$ binding is mainly driven by hydrogen bonding and stacking interactions[27]. Specifically, out of the ten potential hydrogen-bonding groups of $PreQ_1$, nine are recognized by the riboswitch[17]. Notably, L2 contains a highly conserved cytidine (C17) that is essential for $PreQ_1$ binding as they form a Watson-

Crick-Franklin (WCF) base pair. Close analogues of $PreQ_1$, such as $PreQ_0$ and guanine, have several fold lower affinities for the riboswitch, demonstrating that other functional groups of $PreQ_1$, including the aminomethyl group, are very relevant for ligand recognition.

Due to the essential role of Q in bacteria, it is thought that development of synthetic ligands for the $PreQ_1$ riboswitch, that can suppress the production of proteins essential for Q synthesis and transport, is of great interest for developing potential new antibiotics. Several $PreQ_1$ analogues and synthetic ligands for the $PreQ_1$ riboswitch have been discovered and investigated[31–33] (for more information, see Chapter 3), some of which are able to mimic $PreQ_1$ function in *in vitro* riboswitch assays. However, these compounds have no reported antibacterial activity, the discovery of new structurally diverse ligands of the $PreQ_1$ riboswitch remains an interesting field of research. In order to find new ligands that can stabilize the pseudoknot conformation of this dynamic RNA tertiary structure, innovative screening methodologies are required.

Previous research has shown that competitive displacement of specific (fluorescent) binders, such as fluorescent intercalators[34], the Tat peptide from the HIV-1-TAR hairpin[35–38] and labelled antisense RNA to simple RNA structures[39], is an effective strategy for identifying small-molecule ligands for relatively simple RNA structures. In this Chapter, a high-throughput competitive binding antisense assay (CB ASsay) was developed to identify small-molecule ligands that bind to $PreQ_1$-I riboswitches (**Figure 2.2**), thereby demonstrating that competitive binding assays can be also developed for more complex (and clinically relevant) RNA structures. The method employs a 3′-donor fluorophore-labelled pseudoknot and a 5′-acceptor fluorophore-labelled antisense oligonucleotide (ASO) that is complementary to the bases at the 3′-end of the PK (comprising stem P2 and a part of loop L3 of the PK). When the PK and ASO are hybridized, the fluorophore donor-acceptor pair is brought into proximity and the fluorescent signal changes. Addition of a PK-binding ligand can stabilize the PK, thereby preventing the ASO from binding, which results in an unchanged fluorescent signal. Targeting the 3′-end of the PK is a deliberate choice, as this part of the riboswitch is the link between the aptamer and expression platform, and finding ligands that stabilize P2 may increase the likelihood of finding biologically active compounds.

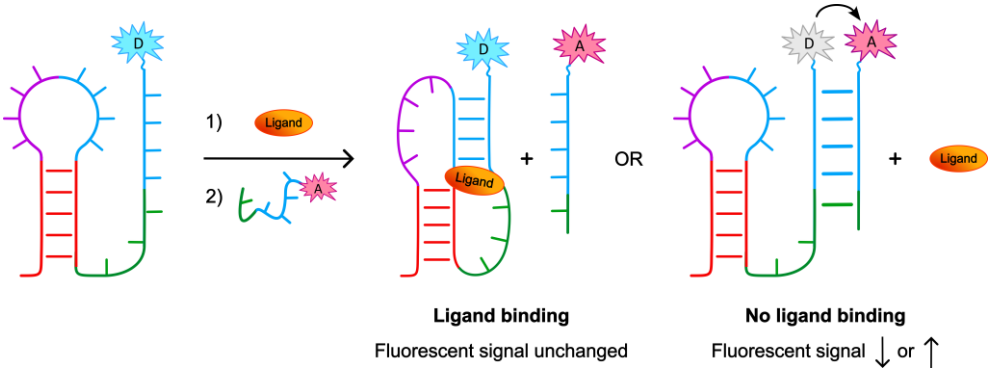

Figure 2.2. Schematic overview of the competitive binding antisense assay (CB ASsay) for the PreQ$_1$ riboswitch. A 3′-donor fluorophore-labelled pseudoknot (PK) is incubated with a potential ligand, after which a 5′-acceptor fluorophore-labelled antisense oligonucleotide (ASO) is added. If a small-molecule ligand binds to the PK, the PK is stabilized and hybridization with the ASO is prevented. In contrast, if the ligand does not bind to the PK, the ASO hybridizes with the PK and changes the fluorescence signal.

In this Chapter, the development of the CB ASsay for PreQ$_1$-I riboswitches is described. First, optimal assay conditions such as antisense length, type of fluorescent labels and buffer composition were determined with the *Fusobacterium nucleatum* (*Fnu*) riboswitch. Subsequently, the CB ASsay was validated by testing PreQ$_1$ and a small library of analogues on several different PreQ$_1$-I riboswitches from *Fnu, Bacillus subtilis* (*Bsu*), *Thermoanaerobacter tengcongensis* (*Tte*) and *Enterococcus faecalis* (*Efa*). Finally, secondary functional assays for hit validation, like translation prevention assays and frameshift assays, were developed. Ultimately, this work functions as a comprehensive workflow for setting up CB ASsays against complex and clinically relevant RNA tertiary structures.

Results

The CB ASsay was developed using the *Fusobacterium nucleatum* (*Fnu*) $PreQ_1$-I riboswitch[28,42], which is a well characterized and clinically relevant target[41,43]. Because the wildtype *Fnu* sequence tends to dimerize, a G7U mutant *Fnu* sequence was employed, which does not form dimers but exhibits similar binding affinity to $PreQ_1$. For ease of reading, this sequence is called *Fnu* wildtype* (WT*) in the rest of the thesis. The *Fnu* PK sequence was first extended at the 3'-end with a d[CCTT] spacer and a terminal fluorescent label (Cy3 or Cy5). Next, antisense oligonucleotides (ASOs) of various lengths were evaluated for their ability to bind to the PK using native polyacrylamide gel electrophoresis (PAGE) (**Figure 2.3A and 2.3B**). It was postulated that the ideal ASO should exhibit approximately 80% binding to the PK at a 1:1 ratio of PK to ASO, thereby allowing sufficient competition with screened ligands while simultaneously ensuring a favourable signal-to-background ratio. From the small library of rationally designed ASOs tested, the shortest ASO fulfilling the 80% binding criterion (ANTI-*Fnu*-GT) was selected as this minimum sequence might be suitable for screening weaker ligands. Then, the selected ANTI-*Fnu*-GT sequence was extended at the 5'-end with either a Cy5 or IowaBlack® RQ (IBRQ) dark quencher (DQ) label, and the CB ASsay was tested with two label-pairs: Cy3-Cy5 and Cy5-IBRQ. For this, the labelled PK was pre-incubated with $PreQ_1$ for 1 hour, followed by the addition of labelled ASO and incubation of an additional 2 hours, after which the fluorescence signal was measured (**Figure 2.3C and 2.3D**).

$PreQ_1$ indeed displays competitive binding behaviour with both label-pairs: upon addition of an increasing concentration of $PreQ_1$, the PK conformation is stabilized, which prevents binding of the ASO and therefore changes the fluorescence signal. However, employing Cy3-Cy5 resulted in a signal-to-background (S/B) ratio of approximately 3, which could not be improved despite adjustments to experimental conditions or excitation and emission wavelengths. In contrast, employing Cy5-IBRQ resulted in a S/B ratio of ~15, providing a clear distinction between the positive and negative controls and thus making it a more suitable system for high-throughput screenings. Therefore, all experiments were performed using the Cy5-IBRQ FRET pair, at room temperature and with a final PK and ASO concentration of 50 nM. To determine the maximal Cy5 signal, a positive control was established by adding a 10-fold excess of unlabelled ASO. Experiments were conducted in a near-physiological buffer[30,44,45] (100 mM Tris (pH = 7.5), 100 mM KCl, 10 mM NaCl, 1 mM $MgCl_2$, 0.1% DMSO and 0.01% Tween20) and the assay showed to be robust towards variations in concentration of individual buffer components (**Figure S2.1**).

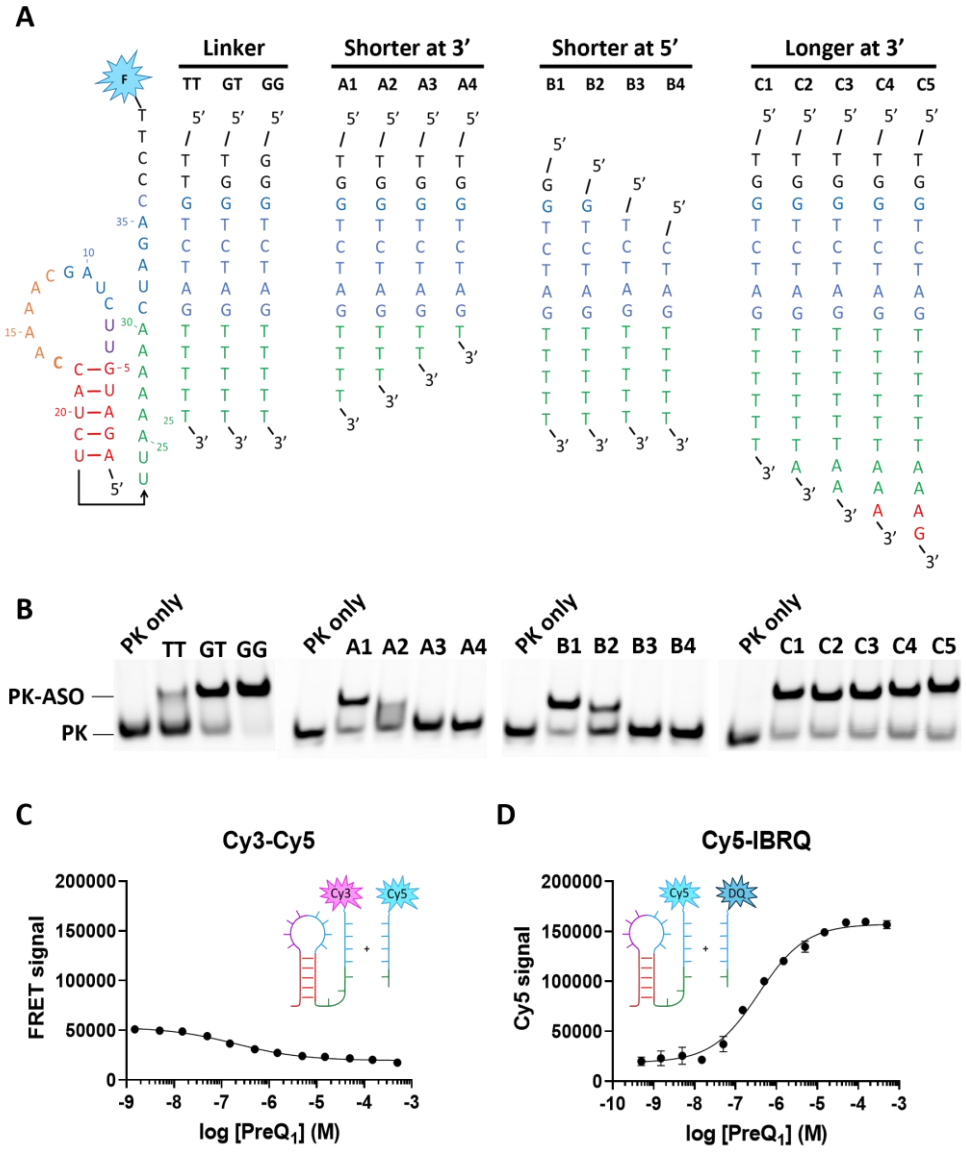

Figure 2.3. A) Antisense oligonucleotide (ASO) sequences screened for the optimisation of the competitive binding antisense assay (CB ASsay) for the *Fusobacterium nucleatum* (*Fnu*) wildtype* (WT*) PreQ$_1$-I riboswitch pseudoknot (PK). **B)** CB ASsay of the *Fnu* PK with different ASO lengths, visualized on a native PAGE. Cy5-PK (1 eq.) was incubated with unlabelled ASO (1 eq.), and the two possible conformations (PK and PK-ASO) were separated on a 20% (w/v) polyacrylamide gel. **C)** CB ASsay of PreQ$_1$ and Cy5-labelled ASO 'ANTI-*Fnu*-GT' to the Cy3-labelled *Fnu* PK. **D)** CB ASsay of PreQ$_1$ and IBRQ-labelled ASO 'ANTI-*Fnu*-GT' to the Cy5-labelled *Fnu* PK.

to promote biologically relevant RNA folding. Moreover, varying the pre-incubation time did not affect the S/B ratio, and the competition between ASO and ligand reached an apparent stable equilibrium 1 hour after ASO addition (**Figure S2.2**), allowing for a reliable readout for subsequent high-throughput screenings.

To test the hypothesis that an ideal ASO should exhibit approximately 80% binding to the PK at a 1:1 ratio of PK to ASO, three ASOs that showed clear differences in binding to the PK (ANTI-*Fnu*-TT, -GT and -GG, **Figure 2.3A and 2.3B**), were re-evaluated in the CB ASsay. These sequences were extended at the 5'-end with a Cy5-label, after which they were tested in the CB ASsay for their ability to compete with $PreQ_1$ for binding to an IBRQ-labelled *Fnu* $PreQ_1$ riboswitch PK (**Figure S2.3**). In the presence of the ANTI-*Fnu*-TT, -GT and -GG ASOs, $PreQ_1$ indeed displays competitive binding behaviour. However, ANTI-*Fnu*-TT shows a low S/B ratio, and ANTI-*Fnu*-GG requires a high concentration of $PreQ_1$ before competitive binding is observed. In contrast, ANTI-*Fnu*-GT shows both a good S/B ratio and a good sensitivity. Based on these results, we confirmed that the 80% binding-rule allows for sufficient competition with screened ligands while simultaneously ensuring a favorable signal-to-background ratio.

Competitive binding of $PreQ_1$ and analogues

To validate the CB ASsay, $PreQ_1$ and various analogues (guanine, adenine, 7-deazaguanine (7dag), 7-carboxy-7-deazaguanine (7c7dag) and 2,6-diaminopurine (2,6dap)) were tested in the competitive binding assay for their ability to stabilize the PK conformation, prevent ASO binding to the *Fnu* WT* riboswitch and retain Cy5 signal (**Figure 2.4A, 2.4C and 2.4D**). Upon addition of PK- stabilizing ligands the Cy5 signal was indeed restored, indicating that the ligands are able to compete with the ASO. For every $PreQ_1$ analogue, the concentration at which the ligand competes with 50% of ASO-PK binding (apparent half-maximal effective concentration, EC_{50}) was determined (**Table 2.1**). In line with literature[17], $PreQ_1$ is the most potent ligand, with an EC_{50} of 0.44 ± 0.07 µM. Close analogues that lack or have a modified aminomethyl group, such as guanine (EC_{50} = 6.9 ± 0.7 µM), 7c7dag (EC_{50} = 23 ± 2.8 µM) and 7dag (EC_{50} = 1301 ± 559 µM), show a lower capacity to bind the *Fnu* riboswitch, as also observed for *Bsu*[17]. Analogues that lack both the aminomethyl group and have modifications in the Watson-Crick-Franklin (WCF) face exhibit no or little competitive binding activity. However, whereas adenine showed no detectable binding, 2,6dap retained some affinity for the *Fnu* riboswitch (EC_{50} = 609 ± 109 µM) as it contains a key exocyclic amine in the WCF face crucial for ligand recognition[17].

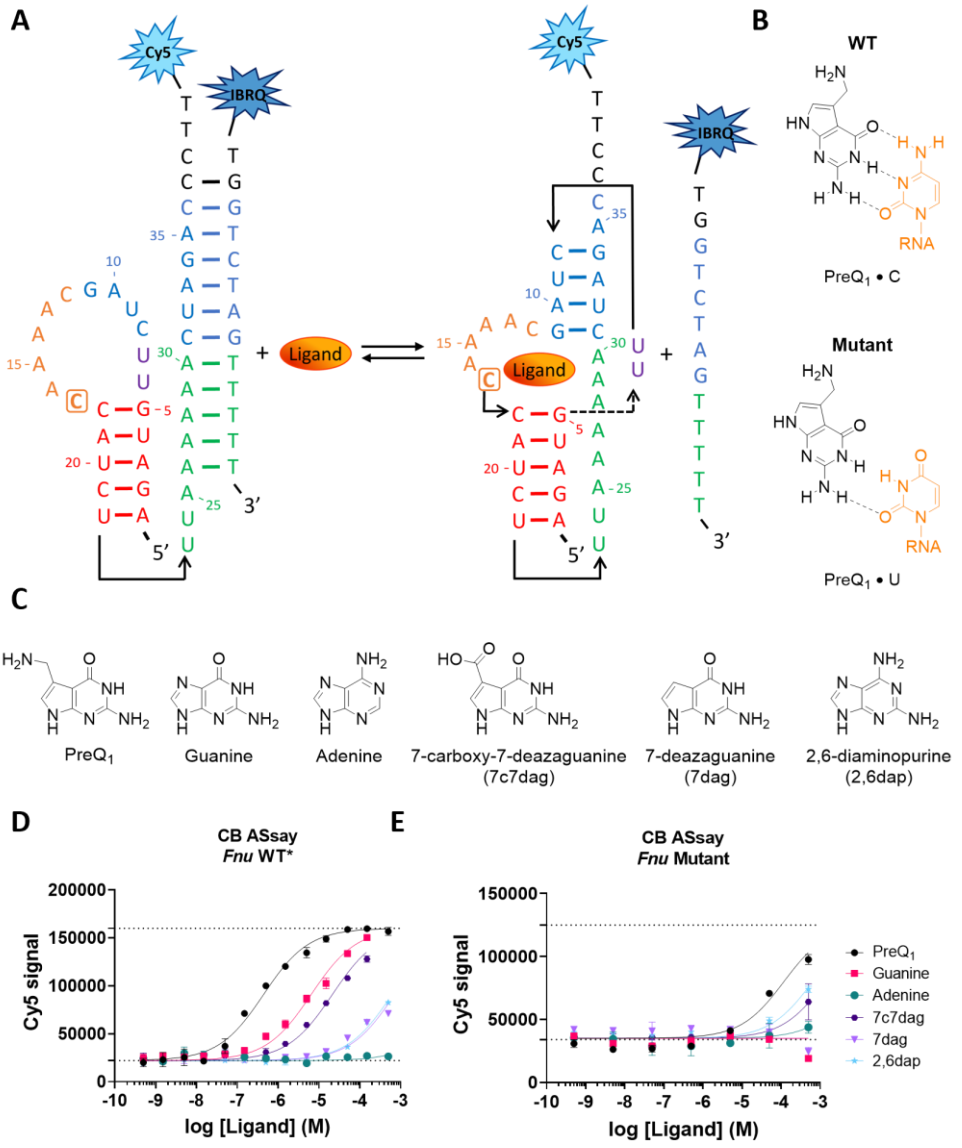

Figure 2.4. Competitive binding antisense assay (CB ASsay) for the *Fusobacterium nucleatum* (*Fnu*) $PreQ_1$-I riboswitch. **A)** Schematic representation of the equilibrium between the Cy5-labelled *Fnu* $PreQ_1$-I riboswitch and IBRQ-labelled antisense oligonucleotide with and without ligand binding. The essential nucleotide C17 is encircled. **B)** Base-pairing of $PreQ_1$ to cytosine (C) or uracil (U). **C)** Molecular structures of $PreQ_1$, guanine, adenine, 7-carboxy-7-deazaguanine (7c7dag), 7-deazaguanine (7dag) and 2,6-diaminopurine (2,6dap). **D-E)** CB ASsay for the *Fnu* wildtype* (WT*) (**D**) or *Fnu* C17U Mutant (**E**) PK with $PreQ_1$ and its analogues. Dotted lines denote the minimum and maximum Cy5 signal as determined by the positive and negative controls. Measurements were performed in duplicate.

Table 2.1. Overview of EC_{50} values from the competitive binding antisense assay (CB ASsay) and apparent K_D values of $PreQ_1$ and its analogues, as determined for the *Fusobacterium nucleatum* (*Fnu*) wildtype* (WT*), the *Thermoanaerobacter tengcongensis* (*Tte*), *Bacillus subtilis* (*Bsu*) and *Enterococcus faecalis* (*Efa*) WT and *Fnu* C17U mutant $PreQ_1$-I riboswitches. ndb = no detectable binding

	Fnu			***Tte***	***Bsu***	***Efa***
	WT*		**Mutant**	**WT**	**WT**	**WT**
	EC_{50} (µM) CB ASsay	**K_D (µM)** MST	**EC_{50} (µM)** CB ASsay	**EC_{50} (µM)** CB ASsay	**EC_{50} (µM)** CB ASsay	**EC_{50} (µM)** CB ASsay
$PreQ_1$	0.44 ± 0.07	0.34 ± 0.03	122 ± 77	0.009 ± 0.002	2.1 ± 0.3	6.1 ± 0.8
Guanine	6.9 ± 0.7	12 ± 1.8	ndb	0.33 ± 0.11	220 ± 69	568 ± 53
Adenine	ndb	>500	>500	ndb	ndb	ndb
7c7dag	23 ± 2.8	11 ± 1.5	>500	0.38 ± 0.12	>500	332 ± 31
7dag	>500	ndb	ndb	2.9 ± 0.9	ndb	ndb
2,6dap	609 ± 109	610 ± 127	>500	30 ± 7.6	>500	ndb

The observed trend in ligand activity with the CB ASsay was further validated through the assessment of their apparent binding affinities to the *Fnu* WT* $PreQ_1$-I riboswitch using microscale thermophoresis (MST) (**Figure S2.4 and Table 2.1**). Coincidentally, the determined apparent K_D and EC_{50} values exhibit good agreement, differing by only a factor of two. Noteworthy is the higher sensitivity of the CB ASsay to weak-binding ligands, particularly evident with 7dag, surpassing the observed sensitivity of MST. For $PreQ_1$, both the apparent K_D and EC_{50} values closely align with the apparent K_D of 0.28 ± 0.055 µM reported in literature[42]. Additionally, the competitive binding between ligand and ASO was further validated with native PAGE (**Figure S2.5**), where upon increasing ligand concentration of $PreQ_1$, guanine and 7c7dag, a clear decrease in ASO-PK complex and increase of PK conformation was observed.

To demonstrate that the recovery of Cy5 signal in the competitive binding assay is driven by ligand occupancy, $PreQ_1$ and its analogues were tested using the *Fnu* C17U mutant PK (**Figure 2.4B, 2.4E and Table 2.1**). The substitution of the cytosine to a uracil reduces $PreQ_1$ affinity due to the disruption of the WCF base pairing[17]. As expected, $PreQ_1$ and other guanine analogues showed a reduced activity with the mutant PK, whereas adenine analogues (adenine and 2,6dap) exhibited similar or increased activity.

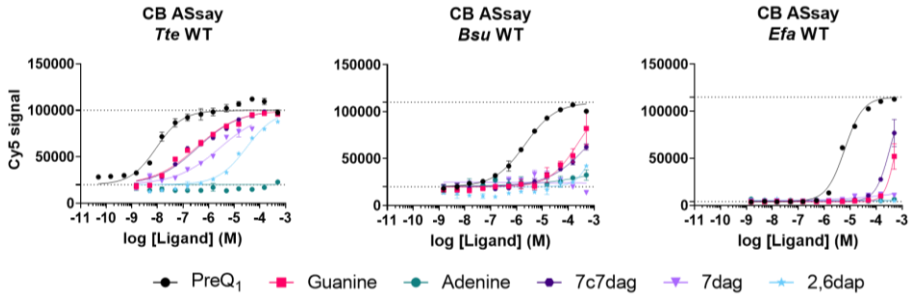

Figure 2.5. Competitive binding antisense assay (CB ASsay) of $PreQ_1$ and its analogues for the *Thermoanaerobacter tengcongensis* (*Tte*), *Bacillus subtilis* (*Bsu*), and *Enterococcus faecalis* (*Efa*) wildtype (WT) PK. Dotted lines denote the minimum and maximum Cy5 signal as determined by the positive and negative controls. All measurements were performed in duplicate.

Expanding the CB ASsay to other $PreQ_1$-I riboswitches

Encouraged by these results, the CB ASsay was extended to the well-studied *Thermoanaerobacter tengcongensis* (*Tte*), *Bacillus subtilis* (*Bsu*) and clinically relevant *Enterococcus faecalis* (*Efa*) $PreQ_1$-I riboswitches. In contrast to the *Fnu* pseudoknot, the second stems of *Tte*, *Bsu* and *Efa* PKs are partially stabilized by non-WCF base pairs, introducing greater complexity to the design of ASO sequences. Fortunately, ASO selection for the *Tte* riboswitch (**Figure S2.6**) was similar to that of *Fnu*, with the PK and PK-ASO complexes separating clearly on native gel and showing length- and linker-dependent binding behaviour. Antisense oligonucleotide ANTI-*Tte*-GGT-3 was selected as it fulfilled the previously postulated 80% binding criterion that worked well for *Fnu*. In contrast, ASO selection for *Bsu* and *Efa* (**Figure S2.7 and S2.8**) proved more difficult, as all PK was bound to the ASO, presumably due to the lower stability of stem P2 of *Bsu* and *Efa* compared to *Fnu*. To assess ASO binding strength, unlabelled ASOs were screened by co-incubating them with Cy5-labelled PKs and increasing concentrations of $PreQ_1$, and their competitive binding was visualized using native PAGE. The ASOs that showed clear, albeit weak, competitive binding upon addition of $PreQ_1$ (ANTI-*Bsu*-GGT-1 and ANTI-*Efa*-GGT-1) were selected.

All selected ASOs were subsequently labelled with a 5'-terminal IBRQ quencher-label and tested with $PreQ_1$ (analogues) in the corresponding CB ASsay (**Figure 2.5**), from which EC_{50} values were determined (**Table 2.1**). The *Tte* riboswitch (apparent K_D of 2 nM for $PreQ_1$)[29] indeed showed high affinity for $PreQ_1$ and its analogues, reaching nanomolar EC_{50} values for $PreQ_1$ and a similar trend in analogue activity as observed for *Fnu*. Notably, for both *Bsu* and *Efa*, the EC_{50} values of $PreQ_1$ are an order of magnitude higher than those observed for *Fnu,* despite $PreQ_1$ having a higher reported binding affinity to the

Bsu riboswitch (K_D = 50 nM)[17] compared to the *Fnu* riboswitch (K_D = 280 ± 55 nM)[42]. The difference between EC_{50} values and reported K_D clearly underscores the influence of both the intrinsic stability of the RNA structure and the binding potency of the ASO to the target sequence on the observed competitive binding activity. These results highlight the importance of appropriately tuning the CB ASsay by adjusting factors such as ASO length, complementarity and/or RNA nucleotide- or backbone modifications for each specific RNA target[39,46]. Interestingly, the Hill slope (which indicates binding stoichiometry) obtained from the dose-response curves of *Fnu*, *Tte* and *Bsu* indicates a 1:1 binding of ligand to riboswitch, whereas the Hill slope of *Efa* identifies a 2:1 binding stoichiometry (**Figure 2.4 and 2.5**). This is in line with previous reports of $PreQ_1$ riboswitches similar to the *Efa* sequence[47], and demonstrates that the CB ASsay provides detailed information about ligand binding.

Translation prevention assay

To evaluate riboswitch ligands on their ability to interfere with RNA function in a biological context, translation prevention and frameshift assays were developed. In the translation prevention assay, the translation of the HiBiT peptide from the NanoBiT® Luciferase, under the regulatory control of the $PreQ_1$ riboswitch, is assessed. Translational control by the riboswitch occurs through the sequestration of the Shine Dalgarno (SD) sequence within the second stem of the pseudoknot, thereby preventing ribosomes from binding and translating the bacterial mRNA (**Figure 2.6A**). For this assay, the *Tte* and *Escherichia coli* (*Eco*) $PreQ_1$-I riboswitches were selected, given their roles as translational regulators in their biological context. After addition of LargeBiT, luciferase activity of the reconstituted NanoBiT® Luciferase was measured and normalized to the DMSO-control.

Upon the addition of $PreQ_1$, translation was reduced by 90% for both the WT and C-to-U Mutant *Tte* and *Eco* riboswitches, albeit that the mutants required a 10 to 100-fold higher concentration of $PreQ_1$ to achieve this effect (**Figure 2.6B**). Notably, the *Tte* riboswitch is more responsive to $PreQ_1$, as this pseudoknot has one of the highest reported affinities for the ligand (apparent K_D = 2.1 ± 0.3 nM)[29]. Addition of guanine, an analogue of $PreQ_1$ that lacks the aminomethyl group, also reduces translation with the *Tte* WT and mutant riboswitches (**Figure 2.6C**), although activity is observed only at 100 to 1000-fold higher concentrations than $PreQ_1$. Guanine does not decrease translation with the *Eco* WT and mutant riboswitches at the tested concentrations. All in all, the observed difference in expression upon addition of either $PreQ_1$ and guanine is both in line with expectation and suitable for screening synthetic ligands for their ability to suppress translation.

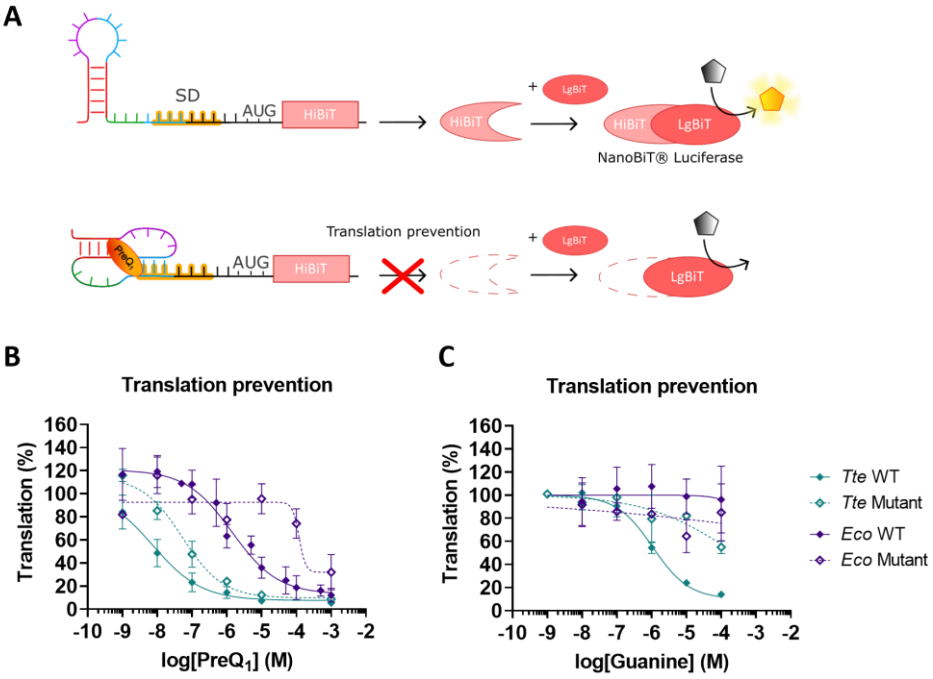

Figure 2.6. Translation prevention assay for the PreQ$_1$ riboswitch. **A)** Schematic overview of the translation prevention assay. The PreQ$_1$ riboswitch regulates the expression of a HiBiT reporter peptide. Without PreQ$_1$, the Shine Dalgarno (SD) sequence is available for ribosomes to bind and start translation, resulting in the production of the NanoBiT luciferase reporter protein. When PreQ$_1$ is present, the riboswitch sequesters the SD sequence and prevents translation. **B-C)** Translation prevention assays of PreQ$_1$ (**B**) and guanine (**C**) with the *Thermoanaerobacter tengcongensis* (*Tte*) and *Escherichia coli* (*Eco*) wildtype (WT) and C→U mutant PreQ$_1$-I riboswitches. Translation percentages are calculated by normalizing the luminescent signal to the DMSO control. Assays were performed in quadruplicate.

Frameshift assay

The $PreQ_1$-I riboswitches of *Fnu* and *Bsu* regulate gene expression through a transcription termination mechanism. Unfortunately, setting up a transcription termination assay was not successful, as no transcription termination was observed even upon addition of high concentrations of $PreQ_1$. Therefore, to test whether ligands can stabilize the pseudoknot structure of $PreQ_1$ riboswitches involved in transcriptional control, a frameshift (FS) assay was set up. This assay, previously validated by Yu *et al.* (2013)[41] using *Fnu*, *Bsu* and *Tte* $PreQ_1$-I riboswitches, measures the increase in –1 ribosomal frameshifting (–1 FS) that is caused by, for example, ligand-induced stabilization of an RNA tertiary structure. A stable RNA tertiary structure can temporarily impede a ribosome from moving along the mRNA, which allows the ribosome to slip into a different reading frame and continue translation to produce an alternative protein product. To evaluate ligand binding, FS assays were carried out with the *Fnu*, *Bsu*, *Tte* and *Eco* $PreQ_1$-I riboswitches that were placed between two parts of the NanoBiT® Luciferase reporter protein gene (**Figure 2.7A**).

The full NanoBiT® luciferase enzyme is only produced upon frameshifting, which was quantified by measuring luminescence signal. This signal was subsequently normalized to an in-frame control to calculate percentage of frameshifting (**Figure 2.7B**). For all riboswitches, addition of $PreQ_1$ indeed increased frameshifting in a dose-dependent manner, although the maximum achieved level of frameshifting varied due to the difference in internal stability of the riboswitches, as previously reported in literature[41]. While the difference in frameshift levels with and without ligand are most pronounced in *Fnu* and *Tte*, the frameshift assay is a useful tool for secondary hit validation for all four riboswitches, including those involved in transcription termination. Of note, high concentrations of $PreQ_1$ inhibited frameshifting, possibly due to overstabilization of the pseudoknot structure.

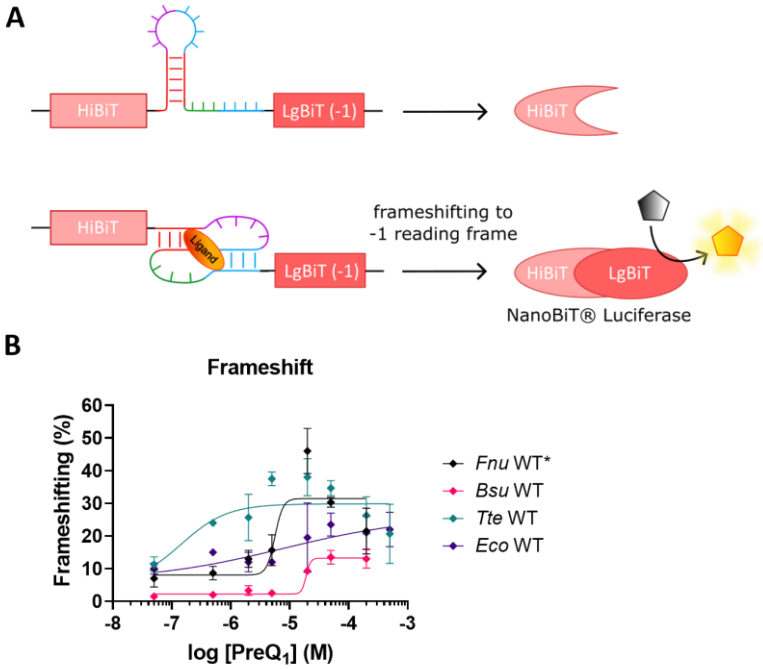

Figure 2.7. Frameshift assay for PreQ$_1$ riboswitches. **A)** Schematic overview of the frameshift assay. The PreQ$_1$ riboswitch is located between two parts of the NanoBiT luciferase reporter protein. Without PreQ$_1$, only the HiBiT peptide is translated. When PreQ$_1$ is present, the pseudoknot conformation is stabilized and induces frameshifting, leading to the translation of the full NanoBiT luciferase reporter protein. **B)** Frameshift assays of PreQ$_1$ with the *Fusobacterium nucleatum* (*Fnu*) wildtype* (WT*) PreQ$_1$-I riboswitch and the *Bacillus subtilis* (*Bsu*), *Thermoanaerobacter tengcongensis* (*Tte*) and *Escherichia coli* (*Eco*) WT PreQ$_1$-I riboswitches. Frameshift percentages are calculated by normalizing the luminescent signal to the in-frame control. Assays were performed in triplicate.

Discussion

In the emerging field of small-molecule RNA targeting, there is a growing demand for new high-throughput screening (HTS) methods. Currently, screenings for targeting RNA are conducted using *in silico*, *in vitro* or *in cellulo* methods. *In silico* approaches, while relatively fast and cost-effective, require high-resolution structural knowledge of the target RNA and are susceptible to false positives and negatives if they cannot accurately account for RNA flexibility[38]. Cellular assays identify biologically active hits, but false positives and negatives can arise from off-target interactions or poor cellular uptake. *In vitro* screening methods make use of purified RNA structures, offering the advantage of circumventing issues with off-target effects, cellular uptake, or lack of structural information. However, many current *in vitro* HTS methods rely on immobilizing the RNA target or small molecules[35,48,49], which can influence the RNA conformation and/or the rotational freedom of the ligand, potentially altering ligand-RNA interactions. Alternatively, *in vitro* competitive displacement assays, that use only in-solution components, have only been successfully applied to relatively simple RNA structures, like hairpins[35–39]. Other methods, including mass spectrometry or nuclear magnetic resonance, can detect low affinity compounds but are susceptible to artifacts or are low throughput, respectively[50]. One successful method that integrates experimental data with *in silico* screening is the 2D combinatorial screening (2DCS), which led to the creation of Inforna database[51]. This database is used to select RNA ligands for relatively simple RNA motifs, while ligands for neighbouring motifs within the RNA target can be assembled into high-affinity hits. While great progress has been made, targeting more complex 3D RNA structures remains a challenge.

In this Chapter, a new *in vitro* and in-solution competitive binding antisense assay (CB ASsay) for targeting more complex tertiary structured RNA is presented. The CB ASsay was developed using the $PreQ_1$-I riboswitch as a model target, which was chosen for its well-studied tertiary structure and binding interactions with its native ligand $PreQ_1$. Moreover, the $PreQ_1$-I riboswitch has an important role in the bacterial biosynthesis pathway of the essential modified nucleobase Queuosine and could therefore be a clinically relevant antibiotic target. For this research, CB ASsays were developed for four structurally and functionally diverse $PreQ_1$-I riboswitch sequences, from *Fusobacterium nucleatum* (*Fnu*), *Thermoanaerobacter tengcongensis* (*Tte*), *Bacillus subtilis* (*Bsu*) and *Enterococcus faecalis* (*Efa*), and the assays were validated with the native ligand $PreQ_1$ and five $PreQ_1$ analogues with known binding properties.

The most important step in the development of the CB ASsay for a new RNA target is selection of the correct antisense oligonucleotide (ASO), which requires certain prior knowledge about RNA secondary structure and function. In the case of the $PreQ_1$-I riboswitch, it is known that the 3'-end of the RNA is the link between the $PreQ_1$ aptamer and the expression platform that regulates gene expression. More specifically, this part of the RNA contains both stem P2 and nucleotides involved in $PreQ_1$ recognition, which are crucial for the correct folding of the pseudoknot conformation and biological function of the riboswitch. Designing an ASO against this part of the RNA structure will likely contribute to finding biologically active ligands.

The optimal ASO length or nucleotide composition was determined with native PAGE. Screening a set of unlabelled ASOs of different lengths or sequence complementarity proved to be a fast and cost-effective method to assess the binding behaviour of different ASOs. It was postulated that a suitable ASO should exhibit an 80% bound – 20% unbound pattern with an equimolar ratio of target to ASO. This pattern indeed yielded a good signal-to-background ratio in the CB ASsay for the *Fnu* and *Tte* $PreQ_1$-I riboswitches and allowed for the detection of weak ligands with high micromolar/low millimolar activity. However, ASO selection for the *Bsu* and *Efa* $PreQ_1$-I riboswitches proved more difficult, as every tested ASO showed complete binding to the RNA structure. This is likely because stem P2 of these RNA structures is intrinsically less stable, giving easy access for the ASOs to bind. Unfortunately, it was not possible to visualize binding of shorter ASOs, as the size difference between PK and PK-ASO became too small for clear separation on gel. Ultimately, ASOs were selected by co-incubation of ASOs with $PreQ_1$ to show competitive binding behaviour. However, this will not be possible for RNA targets without a positive control ligand.

The CB ASsay was tested with two different label pairs: a Cy3-Cy5 FRET pair and a Cy5-IowaBlack® RQ (IBRQ) fluorophore-dark quencher pair. Due to its significantly higher signal-to-background ratio, the Cy5-IBRQ pair was selected for further research. An added benefit is that this fluorophore-quencher pair eliminates the use of Cy3, an orange-fluorescent dye that is more susceptible to compound interference than the further red-shifted Cy5[52]. This is especially relevant for RNA targeting, because RNA ligands often contain aromatic rings or more extended conjugated systems that can interact with light, either through autofluorescence or quenching[53], leading to a higher number of false positives and negatives. Employing red-shifted fluorophores like Cy5 helps with reducing compound interference and will improve the data quality of future HTS campaigns.

$PreQ_1$ showed competitive binding activity with all four riboswitches, with EC_{50} values in the nanomolar (*Tte*) to micromolar (*Fnu*, *Bsu*, *Efa*) range. Interestingly, the competitive binding activity of $PreQ_1$ to the *Fnu* riboswitch (EC_{50} = 0.44 ± 0.07 µM) is within a factor 2 of the previously reported apparent binding affinity (K_D = 0.28 ± 0.055 µM)[42]. For *Tte,* the CB activity (EC_{50} = 9 ± 2 nM) differs only a factor 5 of the binding affinity (K_D = 2.1 ± 0.3 nM)[29]. However, for the *Bsu* riboswitch, there is a clear disparity between the CB activity (EC_{50} = 2.1 ± 0.3 µM) and binding affinity (K_D = 50 nM)[17]. This difference is likely caused by both the lower intrinsic stability of the *Bsu* riboswitch and the relatively high binding potency of the ASO. By taking into account these factors, it should be possible to estimate ligand affinity from the measured CB activity. Moreover, tuning the ASO binding strength by changing its length or nucleotide composition could help with decreasing the assay stringency to detect weaker ligands.

It is important to note that the CB ASsay is an artificial biochemical assay, meaning that the assay conditions do not perfectly replicate a biological system. Differences in natural context of the target RNA, including flanking RNA sequences and cellular environment, may lead to alternative RNA (folding) conformations or ligand-binding behaviour. Secondary assays for hit validation to confirm ligand-target interactions in a biological environment, along with validation by functional or biological assays, are highly recommended. In this Chapter, a translation prevention assay and a frameshift assay were set-up. The translation prevention assay is used to assess riboswitch-mediated gene regulation with the *Tte* and *Escherichia coli* (*Eco)* riboswitches, as this is their function in a natural context. Indeed, translation was significantly reduced upon addition of $PreQ_1$ and guanine, with a correlation between ligand affinity and effective concentration. However, the translation prevention assay is not suitable for the *Fnu* and *Bsu* riboswitches, as their natural mechanism for gene regulation is transcription termination.

As setting up a transcription termination assay was not successful, a frameshift assay measuring ligand-induced pseudoknot structure stabilization was employed. Through this assay, $PreQ_1$-induced frameshifting for both transcription regulators (*Fnu* and *Bsu*) and translation regulators (*Tte* and *Eco*) was observed, making it a valuable secondary hit validation assay. Moreover, since the frameshift assay is a turn-on assay, *i.e.* showing a signal increase, it will less likely be affected by general toxicity of compounds as compared to the translation prevention assay. Thus, the combination of both assays for hit validation will be a good assessment of ligand-RNA interactions.

All in all, the assays developed in this Chapter provide a comprehensive screening-to-lead platform to find new RNA ligands. Most importantly, the here-developed CB ASsay is able to detect ligands for $PreQ_1$-I pseudoknots, which is the first reported *in vitro* and in-solution competitive binding assay developed for an RNA tertiary structure. This CB ASsay can be easily upscaled to perform high-throughput screenings (see Chapter 3) and is applicable to other RNA tertiary structures as illustrated in Chapter 4 and 5.

Acknowledgements

Mariska Tacoma is acknowledged for the development of the translation prevention assay of the *Eco* WT and mutant $PreQ_1$-I riboswitches, and the assessment of the binding behaviour of antisense oligonucleotides against the *Fnu* $PreQ_1$-I riboswitch. Indy Broekhuizen is acknowledged for the development of the frameshift assays for the *Fnu* WT*, *Fnu* mutant, *Bsu* and *Efa* $PreQ_1$-I riboswitches and the evaluation of the binding behaviour of $PreQ_1$ analogues to the *Fnu* WT* $PreQ_1$-I riboswitch on native PAGE.

References

(1) Oldfield, C. J.; Cheng, Y.; Cortese, M. S.; Brown, C. J.; Uversky, V. N.; Dunker, A. K. Comparing and Combining Predictors of Mostly Disordered Proteins. *Biochemistry* **2005**, *44* (6), 1989–2000. https://doi.org/10.1021/bi047993o.

(2) Haniff, H. S.; Knerr, L.; Chen, J. L.; Disney, M. D.; Lightfoot, H. L. Target-Directed Approaches for Screening Small Molecules against RNA Targets. *SLAS Discov. Adv. Sci. Drug Discov.* **2020**, *25* (8), 869–894. https://doi.org/10.1177/2472555220922802.

(3) Warner, K. D.; Hajdin, C. E.; Weeks, K. M. Principles for Targeting RNA with Drug-like Small Molecules. *Nat. Rev. Drug Discov.* **2018**, *17* (8), 547–558. https://doi.org/10.1038/nrd.2018.93.

(4) Hong, W.; Zeng, J.; Xie, J. Antibiotic Drugs Targeting Bacterial RNAs. *Acta Pharm. Sin. B* **2014**, *4* (4), 258–265. https://doi.org/10.1016/j.apsb.2014.06.012.

(5) Lünse, C. E.; Schüller, A.; Mayer, G. The Promise of Riboswitches as Potential Antibacterial Drug Targets. *Int. J. Med. Microbiol.* **2014**, *304* (1), 79–92. https://doi.org/10.1016/j.ijmm.2013.09.002.

(6) Mandal, M.; Breaker, R. R. Gene Regulation by Riboswitches. *Nat. Rev. Mol. Cell Biol.* **2004**, *5* (6), 451–463. https://doi.org/10.1038/nrm1403.

(7) Tucker, B. J.; Breaker, R. R. Riboswitches as Versatile Gene Control Elements. *Curr. Opin. Struct. Biol.* **2005**, *15* (3), 342–348. https://doi.org/10.1016/j.sbi.2005.05.003.

(8) Serganov, A.; Nudler, E. A Decade of Riboswitches. *Cell* **2013**, *152* (1), 17–24. https://doi.org/10.1016/j.cell.2012.12.024.

(9) Garst, A. D.; Edwards, A. L.; Batey, R. T. Riboswitches: Structures and Mechanisms. *Cold Spring Harb. Perspect. Biol.* **2011**, *3* (6), a003533. https://doi.org/10.1101/cshperspect.a003533.

(10) Breaker, R. R. The Biochemical Landscape of Riboswitch Ligands. *Biochemistry* **2022**, *61* (3), 137–149. https://doi.org/10.1021/acs.biochem.1c00765.

(11) Harada, F.; Nishimura, S. Possible Anticodon Sequences of tRNAHis, tRNAAsn, and tRNAAsp from Escherichia Coli. Universal Presence of Nucleoside O in the First Position of the Anticodons of These Transfer Ribonucleic Acid. *Biochemistry* **1972**, *11* (2), 301–308. https://doi.org/10.1021/bi00752a024.

(12) Hillmeier, M.; Wagner, M.; Ensfelder, T.; Korytiakova, E.; Thumbs, P.; Müller, M.; Carell, T. Synthesis and Structure Elucidation of the Human tRNA Nucleoside Mannosyl-Queuosine. *Nat. Commun.* **2021**, *12* (1), 7123. https://doi.org/10.1038/s41467-021-27371-9.

(13) Iwata-Reuyl, D. Biosynthesis of the 7-Deazaguanosine Hypermodified Nucleosides of Transfer RNA. *Bioorganic Chem.* **2003**, *31* (1), 24–43. https://doi.org/10.1016/S0045-2068(02)00513-8.

(14) Meier, F.; Suter, B.; Grosjean, H.; Keith, G.; Kubli, E. Queuosine Modification of the Wobble Base in tRNAHis Influences 'in Vivo' Decoding Properties. *EMBO J.* **1985**, *4* (3), 823–827. https://doi.org/10.1002/j.1460-2075.1985.tb03704.x.

(15) Durand, J. M. B.; Dagberg, B.; Uhlin, B. E.; Björk, G. R. Transfer RNA Modification, Temperature and DNA Superhelicity Have a Common Target in the Regulatory Network of the Virulence of Shigella Flexneri: The Expression of the virF Gene. *Mol. Microbiol.* **2000**, *35* (4), 924–935. https://doi.org/10.1046/j.1365-2958.2000.01767.x.

(16) Noguchi, S.; Nishimura, Y.; Hirota, Y.; Nishimura, S. Isolation and Characterization of an Escherichia Coli Mutant Lacking tRNA-Guanine Transglycosylase. Function and Biosynthesis of Queuosine in tRNA. *J. Biol. Chem.* **1982**, *257* (11), 6544–6550. https://doi.org/10.1016/S0021-9258(20)65176-6.

(17) Roth, A.; Winkler, W. C.; Regulski, E. E.; Lee, B. W. K.; Lim, J.; Jona, I.; Barrick, J. E.; Ritwik, A.; Kim, J. N.; Welz, R.; Iwata-Reuyl, D.; Breaker, R. R. A Riboswitch Selective for the Queuosine Precursor preQ1 Contains an Unusually Small Aptamer Domain. *Nat. Struct. Mol. Biol.* **2007**, *14* (4), 308–317. https://doi.org/10.1038/nsmb1224.

(18) Eichhorn, C. D.; Kang, M.; Feigon, J. Structure and Function of preQ1 Riboswitches. *Biochim. Biophys. Acta BBA - Gene Regul. Mech.* **2014**, *1839* (10), 939–950. https://doi.org/10.1016/j.bbagrm.2014.04.019.

(19) McCarty, R. M.; Bandarian, V. Biosynthesis of Pyrrolopyrimidines. *Bioorganic Chem.* **2012**, *43*, 15–25. https://doi.org/10.1016/j.bioorg.2012.01.001.

(20) Meyer, M. M.; Roth, A.; Chervin, S. M.; Garcia, G. A.; Breaker, R. R. Confirmation of a Second Natural preQ1 Aptamer Class in Streptococcaceae Bacteria. *RNA* **2008**, *14* (4), 685–695. https://doi.org/10.1261/rna.937308.

(21) McCown, P. J.; Liang, J. J.; Weinberg, Z.; Breaker, R. R. Structural, Functional, and Taxonomic Diversity of Three PreQ1 Riboswitch Classes. *Chem. Biol.* **2014**, *21* (7), 880–889. https://doi.org/10.1016/j.chembiol.2014.05.015.

(22) Kim, J. N.; Breaker, R. R. Purine Sensing by Riboswitches. *Biol. Cell* **2008**, *100* (1), 1–11. https://doi.org/10.1042/BC20070088.

(23) Blount, K. F.; Breaker, R. R. Riboswitches as Antibacterial Drug Targets. *Nat. Biotechnol.* **2006**, *24* (12), 1558–1564. https://doi.org/10.1038/nbt1268.

(24) Pavlova, N.; Penchovsky, R. Bioinformatics and Genomic Analyses of the Suitability of Eight Riboswitches for Antibacterial Drug Targets. *Antibiotics* **2022**, *11* (9), 1177. https://doi.org/10.3390/antibiotics11091177.

(25) Pavlova, N.; Kaloudas, D.; Penchovsky, R. Riboswitch Distribution, Structure, and Function in Bacteria. *Gene* **2019**, *708*, 38–48. https://doi.org/10.1016/j.gene.2019.05.036.

(26) Pleij, C. W. A.; Rietveld, K.; Bosch, L. A New Principle of RNA Folding Based on Pseudoknotting. *Nucleic Acids Res.* **1985**, *13* (5), 1717–1731. https://doi.org/10.1093/nar/13.5.1717.

(27) Klein, D. J.; Edwards, T. E.; Ferré-D'Amaré, A. R. Cocrystal Structure of a Class I preQ1 Riboswitch Reveals a Pseudoknot Recognizing an Essential Hypermodified Nucleobase. *Nat. Struct. Mol. Biol.* **2009**, *16* (3), 343–344. https://doi.org/10.1038/nsmb.1563.

(28) Rieder, U.; Lang, K.; Kreutz, C.; Polacek, N.; Micura, R. Evidence for Pseudoknot Formation of Class I preQ1 Riboswitch Aptamers. *ChemBioChem* **2009**, *10* (7), 1141–1144. https://doi.org/10.1002/cbic.200900155.

(29) Jenkins, J. L.; Krucinska, J.; McCarty, R. M.; Bandarian, V.; Wedekind, J. E. Comparison of a PreQ1 Riboswitch Aptamer in Metabolite-Bound and Free States with Implications for Gene Regulation *. *J. Biol. Chem.* **2011**, *286* (28), 24626–24637. https://doi.org/10.1074/jbc.M111.230375.

(30) Suddala, K. C.; Rinaldi, A. J.; Feng, J.; Mustoe, A. M.; Eichhorn, C. D.; Liberman, J. A.; Wedekind, J. E.; Al-Hashimi, H. M.; Brooks, C. L.; Walter, N. G. Single Transcriptional and Translational preQ1 Riboswitches Adopt Similar Pre-Folded Ensembles That Follow Distinct Folding Pathways into the Same Ligand-Bound Structure. *Nucleic Acids Res.* **2013**, *41* (22), 10462–10475. https://doi.org/10.1093/nar/gkt798.

(31) Connelly, C. M.; Numata, T.; Boer, R. E.; Moon, M. H.; Sinniah, R. S.; Barchi, J. J.; Ferré-D'Amaré, A. R.; Schneekloth, J. S. Synthetic Ligands for PreQ1 Riboswitches Provide Structural and Mechanistic Insights into Targeting RNA Tertiary Structure. *Nat. Commun.* **2019**, *10* (1), 1501. https://doi.org/10.1038/s41467-019-09493-3.

(32) Neuner, E.; Frener, M.; Lusser, A.; Micura, R. Superior Cellular Activities of Azido- over Amino-Functionalized Ligands for Engineered preQ1 Riboswitches in E.Coli. *RNA Biol.* **2018**, *15* (10), 1376–1383. https://doi.org/10.1080/15476286.2018.1534526.

(33) Kallert, E.; Fischer, T. R.; Schneider, S.; Grimm, M.; Helm, M.; Kersten, C. Protein-Based Virtual Screening Tools Applied for RNA–Ligand Docking Identify New Binders of the preQ1-Riboswitch. *J. Chem. Inf. Model.* **2022**, *62* (17), 4134–4148. https://doi.org/10.1021/acs.jcim.2c00751.

(34) Wicks, S. L.; Hargrove, A. E. Fluorescent Indicator Displacement Assays to Identify and Characterize Small Molecule Interactions with RNA. *Methods* **2019**, *167*, 3–14. https://doi.org/10.1016/j.ymeth.2019.04.018.

(35) Mei, H.-Y.; Mack, D. P.; Galan, A. A.; Halim, N. S.; Heldsinger, A.; Loo, J. A.; Moreland, D. W.; Sannes-Lowery, K. A.; Sharmeen, L.; Truong, H. N.; Czarnik, A. W. Discovery of Selective, Small-Molecule Inhibitors of RNA Complexes—1. The Tat Protein/TAR RNA Complexes Required for HIV-1 Transcription. *Bioorg. Med. Chem.* **1997**, *5* (6), 1173–1184. https://doi.org/10.1016/S0968-0896(97)00064-3.

(36) Gelus, N.; Bailly, C.; Hamy, F.; Klimkait, T.; Wilson, W. D.; Boykin, D. W. Inhibition of HIV-1 Tat-TAR Interaction by Diphenylfuran Derivatives: Effects of the Terminal Basic Side Chains. *Bioorg. Med. Chem.* **1999**, *7* (6), 1089–1096. https://doi.org/10.1016/S0968-0896(99)00041-3.

(37) Patwardhan, N. N.; Cai, Z.; Newson, C. N.; Hargrove, A. E. Fluorescent Peptide Displacement as a General Assay for Screening Small Molecule Libraries against RNA. *Org. Biomol. Chem.* **2019**, *17* (7), 1778–1786. https://doi.org/10.1039/C8OB02467G.

(38) Ganser, L. R.; Lee, J.; Rangadurai, A.; Merriman, D. K.; Kelly, M. L.; Kansal, A. D.; Sathyamoorthy, B.; Al-Hashimi, H. M. High-Performance Virtual Screening by Targeting a High-Resolution RNA Dynamic Ensemble. *Nat. Struct. Mol. Biol.* **2018**, *25* (5), 425–434. https://doi.org/10.1038/s41594-018-0062-4.

(39) Menichelli, E.; Lam, B. J.; Wang, Y.; Wang, V. S.; Shaffer, J.; Tjhung, K. F.; Bursulaya, B.; Nguyen, T. N.; Vo, T.; Alper, P. B.; McAllister, C. S.; Jones, D. H.; Spraggon, G.; Michellys, P.-Y.; Joslin, J.; Joyce, G. F.; Rogers, J. Discovery of Small Molecules That Target a Tertiary-Structured RNA. *Proc. Natl. Acad. Sci.* **2022**, *119* (48), e2213117119. https://doi.org/10.1073/pnas.2213117119.

(40) Dilweg, I. W.; Oskam, M. G.; Overbeek, S.; Olsthoorn, R. C. L. Investigating the Correlation between Xrn1-Resistant RNAs and Frameshifter Pseudoknots. *RNA Biol.* **2023**, *20* (1), 409–418. https://doi.org/10.1080/15476286.2023.2205224.

(41) Yu, C.-H.; Luo, J.; Iwata-Reuyl, D.; Olsthoorn, R. C. L. Exploiting preQ1 Riboswitches To Regulate Ribosomal Frameshifting. *ACS Chem. Biol.* **2013**, *8* (4), 733–740. https://doi.org/10.1021/cb300629b.

(42) Rieder, U.; Kreutz, C.; Micura, R. Folding of a Transcriptionally Acting PreQ1 Riboswitch. *Proc. Natl. Acad. Sci.* **2010**, *107* (24), 10804–10809. https://doi.org/10.1073/pnas.0914925107.

(43) Chen, Y.; Huang, Z.; Tang, Z.; Huang, Y.; Huang, M.; Liu, H.; Ziebolz, D.; Schmalz, G.; Jia, B.; Zhao, J. More Than Just a Periodontal Pathogen –the Research Progress on Fusobacterium Nucleatum. *Front. Cell. Infect. Microbiol.* **2022**, *12*, 815318. https://doi.org/10.3389/fcimb.2022.815318.

(44) Leamy, K. A.; Assmann, S. M.; Mathews, D. H.; Bevilacqua, P. C. Bridging the Gap between in Vitro and in Vivo RNA Folding. *Q. Rev. Biophys.* **2016**, *49*. https://doi.org/10.1017/S003358351600007X.

(45) Feig, A. L.; Uhlenbeck, O. C. The Role of Metal Ions in RNA Biochemistry. *Cold Spring Harb. Monogr. Ser.* **1999**, *37*, 287–320.

(46) Braasch, D. A.; Corey, D. R. Locked Nucleic Acid (LNA): Fine-Tuning the Recognition of DNA and RNA. *Chem. Biol.* **2001**, *8* (1), 1–7. https://doi.org/10.1016/S1074-5521(00)00058-2.

(47) Schroeder, G. M.; Cavender, C. E.; Blau, M. E.; Jenkins, J. L.; Mathews, D. H.; Wedekind, J. E. A Small RNA That Cooperatively Senses Two Stacked Metabolites in One Pocket for Gene Control. *Nat. Commun.* **2022**, *13* (1), 199. https://doi.org/10.1038/s41467-021-27790-8.

(48) Chen, C. Z.; Sobczak, K.; Hoskins, J.; Southall, N.; Marugan, J. J.; Zheng, W.; Thornton, C. A.; Austin, C. P. Two High-throughput Screening Assays for Aberrant RNA-Protein Interactions in Myotonic Dystrophy Type-1. *Anal. Bioanal. Chem.* **2012**, *402* (5), 1889–1898. https://doi.org/10.1007/s00216-011-5604-0.

(49) Disney, M. D.; Labuda, L. P.; Paul, D. J.; Poplawski, S. G.; Pushechnikov, A.; Tran, T.; Velagapudi, S. P.; Wu, M.; Childs-Disney, J. L. Two-Dimensional Combinatorial Screening Identifies Specific Aminoglycoside−RNA Internal Loop Partners. *J. Am. Chem. Soc.* **2008**, *130* (33), 11185–11194. https://doi.org/10.1021/ja803234t.

(50) Martin, W. J.; Grandi, P.; Marcia, M. Screening Strategies for Identifying RNA- and Ribonucleoprotein-Targeted Compounds. *Trends Pharmacol. Sci.* **2021**, *42* (9), 758–771. https://doi.org/10.1016/j.tips.2021.06.001.

(51) Disney, M. D.; Winkelsas, A. M.; Velagapudi, S. P.; Southern, M.; Fallahi, M.; Childs-Disney, J. L. Inforna 2.0: A Platform for the Sequence-Based Design of Small Molecules Targeting Structured RNAs. *ACS Chem. Biol.* **2016**, *11* (6), 1720–1728. https://doi.org/10.1021/acschembio.6b00001.

(52) Turek-Etienne, T. C.; Small, E. C.; Soh, S. C.; Xin, T. A.; Gaitonde, P. V.; Barrabee, E. B.; Hart, R. F.; Bryant, R. W. Evaluation of Fluorescent Compound Interference in 4 Fluorescence Polarization Assays: 2 Kinases, 1 Protease, and 1 Phosphatase. *SLAS Discov.* **2003**, *8* (2), 176–184. https://doi.org/10.1177/1087057103252304.

(53) Simeonov, A.; Davis, M. I. Interference with Fluorescence and Absorbance. In *Assay Guidance Manual*; Eli Lilly & Company and the National Center for Advancing Translational Sciences: Bethesda (MD), 2004.

Materials & Methods

Materials. All labelled oligonucleotides (**Table S2.1**) were ordered from Sigma-Aldrich or IDT and were HPLC purified. All unlabelled oligonucleotides (**Table S2.1-S2.3**) were purchased from Sigma-Aldrich in desalted format and were used without further purification. All used materials were certified DNAse and RNAse free.

Competitive binding antisense assay (CB ASsay). For all CB ASsays, Cy5-labelled $PreQ_1$ riboswitch (Cy5-PK) and IowaBlack® RQ-labelled antisense oligonucleotide (IBRQ-ASO) were dissolved and diluted to 1 µM in milli-Q water. All ligands were dissolved in DMSO. Positive control: a 10-fold excess of unlabelled ASO. Negative control: DMSO. All CB experiments were carried out in a CB buffer (100 mM Tris (pH=7.6), 100 mM KCl, 10 mM NaCl, 1 mM $MgCl_2$, 0.1% DMSO and 0.01% Tween20).

In a typical CB ASsay, 0.5 µL of ligand (dissolved in DMSO) was pipetted into a black 384-wells plate (Greiner Bio-One, Small Volume, 784076). To this, a mixture containing 0.5 µL of 1 µM Cy5-PK solution (in milli-Q water) and 6.5 µL of CB buffer was added, and the mixture was incubated at RT for 1 h. After this, a mixture containing 0.5 µL of 1 µM IBRQ-ASO and 2.5 µL CB buffer was added, after which the mixture was mixed by pipetting up and down and subsequently incubated at RT for 2 h. The fluorescence was measured with a CLARIOstar (BMG LABTECH) using λ_{ex} = 610 ± 30 nm, λ_{em} = 675 ± 50 nm, gain = 2200 and focal point = 10.2. Obtained fluorescent signals were plotted against ligand concentration. EC_{50} values were determined in GraphPad Prism 8 using the '[Inhibitor] *versus* response – Variable slope (four parameters)' analysis with Bottom constraint = average of DMSO control and Top constraint = average of 10-fold excess unlabelled ASO.

CB ASsay on native gel electrophoresis. Cy5-labelled $PreQ_1$ riboswitch (Cy5-PK) and unlabelled antisense oligonucleotide (unl. ASO) were dissolved and diluted to 10 µM in milli-Q water. All ligands were dissolved in DMSO. In all experiments, a 10x CB buffer (1 M Tris (pH=7.6), 1 M KCl, 100 mM NaCl, 10 mM $MgCl_2$, 1% DMSO and 0.1% Tween20) was used. To an Eppendorf tube was added 0.5 µL of 10 µM Cy5-PK solution, 3 µL milli-Q water, 0.5 µL of 10x CB buffer and 0.5 µL ligand, which was incubated at RT for 30 min. To this, 0.5 µL of 10 µM unl. ASO was added, and the mixture was incubated at RT for 10 min. Different RNA conformations were separated on a 20% native polyacrylamide gel at 4 °C and bands were visualized on a GelDoc (Bio-Rad) and processed using Image Lab software (Bio-Rad).

Microscale thermophoresis (MST). Cy5-labelled *Fnu* WT* $PreQ_1$ riboswitch (Cy5-PK) was diluted to 80 nM in CB buffer (100 mM Tris (pH=7.6), 100 mM KCl, 10 mM NaCl, 1 mM $MgCl_2$, 0.1% DMSO and 0.01% Tween20). A two-fold dilution series of ligand in buffer + DMSO was prepared, maintaining a final DMSO concentration of 5%. To each ligand concentration, an equal volume of diluted Cy5-PK was added, resulting in a final Cy5-PK concentration of 40 nM and ligand concentrations ranging from 15.3 nM to 500 µM. Samples were incubated at RT for 15 min, after which the samples were transferred to standard coated capillaries (NanoTemper Technologies) and subsequently subjected to MST analysis. MST experiments were conducted in triplicate on a Monolith NT.115 system (NanoTemper Technologies). The results were analysed with MO.Affinity Analysis v2.1.5 software, and the obtained 'Fraction bound' values were plotted against ligand concentrations. The apparent dissociation constants were determined in GraphPad Prism 8 using the '[Inhibitor] *vs* response – variable slope (four parameters)' analysis with Bottom constraint = 0 and Top constraint = 1.

Translation prevention assay. DNA constructs containing a T7 promotor, a $PreQ_1$ riboswitch and the sequence of HiBiT Nano Luciferase (**Table S2.2**) were obtained from full-length primers (Sigma-Aldrich) that were annealed and amplified by PCR. Transcripts were synthesized by T7 RNA polymerase (NEB T7 high yield RNA synthesis kit) and were not purified before use. To 0.5 µL of approximately 20 ng/µL RNA was added 1 µL ligand (dissolved in 5% DMSO). Next, 0.5 µL PURExpress® Solution A (New England Biolabs), 0.375 µL PURExpress® Solution B and 2.625 µL dilution buffer (10 mM Tris (pH=7.5), 202 mM KOAc, 15 mM $Mg(OAc)_2$) were added, and the mixture was incubated for 30 min at 37 ˚C (final concentration DMSO was 2%). The reaction was quenched with 10 mM Tris-HCl (pH=7.5) and supplemented with LgBiT Protein (Promega). The solution was transferred into a white 96-wells plate and 2.5 µL of Nano-Glo® substrate (Promega) was added. Luminescence was measured on a GloMax Multi+ Detection System (Promega) and normalized to the DMSO control.

Frameshift assay. $PreQ_1$ riboswitches were cloned into SpeI-HindIII digested plasmid pMOFS as decribed in Dilweg, Oskam *et al.* (2023)[40] (**Table S2.3**). This plasmid produces functional nanoluciferase when –1 frameshifting takes place. To enhance frameshifting, stem P1 of the $PreQ_1$ pseudoknots was replaced by five GC base pairs as reported by Yu *et al.* (2013)[41]. In addition, the length and composition of loop L3 were modified to adjust the reading frame. Transcripts were synthesized by T7 RNA polymerase (NEB T7 high yield RNA synthesis kit) using PCR templates obtained by amplification with primers T7sm-g and pucrev3. Synthesized RNA was diluted to an approximate concentration of 10 ng/µL

and 0.5 µL was incubated with 0.5 µL ligand (dissolved in 8% DMSO in milli-Q water) for 15 min at RT. Subsequently, 1 µL rabbit reticulocyte lysate (Nuclease-treated, Promega) was added and incubated at 28 °C for 45 min (final concentration DMSO was 2%). The reaction was quenched with 10 mM Tris-HCl (pH=7.5) and transferred to a white 96-wells plate, to which 2.5 µL of 100x diluted Nano-Glo® HiBiT Lytic Substrate (Promega) was added. Luminescence was measured on a GloMax Multi+ Detection System (Promega) and data were normalized to an in-frame control.

Supplementary Information

Table S2.1. Sequences of the **competitive binding antisense assay (CB ASsay)**. RNA indicated in black. Linker (DNA) indicated in red. DNA indicated in blue. Mutated bases are underlined.

Name	Sequence (5′ → 3′)
Cy5-PrQ-FnuWT*	AGAUGUUCUAGCAAAACCAUCUUUAAAAAACUAGACCCTT[Cy5]
Cy3-PrQ-FnuWT*	AGAUGUUCUAGCAAAACCAUCUUUAAAAAACUAGACCCTT[Cy3]
IBRQ-PrQ-FnuWT*	AGAUGUUCUAGCAAAACCAUCUUUAAAAAACUAGACCCTT[IBRQ]
Cy5-PrQ-FnuMut	AGAUGUUCUAGCAAAAUCAUCUUUAAAAAACUAGACCCTT[Cy5]
IRBQ-ANTI-PrQFnu	[IBRQ]TGGTCTAGTTTTT
Cy5-ANTI-Fnu-TT	[Cy5]TTGTCTAGTTTTT
Cy5-ANTI-Fnu-GT	[Cy5]TGGTCTAGTTTTT
Cy5-ANTI-Fnu-GG	[Cy5]GGGTCTAGTTTTT
ANTI-Fnu-TT	TTGTCTAGTTTTT
ANTI-Fnu-GT	TGGTCTAGTTTTT
ANTI-Fnu-GG	GGGTCTAGTTTTT
ANTI-Fnu-A1	TGGTCTAGTTTT
ANTI-Fnu-A2	TGGTCTAGTTT
ANTI-Fnu-A3	TGGTCTAGTT
ANTI-Fnu-A4	TGGTCTAGT
ANTI-Fnu-B1	GGTCTAGTTTTT
ANTI-Fnu-B2	GTCTAGTTTTT
ANTI-Fnu-B3	TCTAGTTTTT
ANTI-Fnu-B4	CTAGTTTTT
ANTI-Fnu-C1	TGGTCTAGTTTTTT
ANTI-Fnu-C2	TGGTCTAGTTTTTTA
ANTI-Fnu-C3	TGGTCTAGTTTTTTAA
ANTI-Fnu-C4	TGGTCTAGTTTTTTAAA
ANTI-Fnu-C5	TGGTCTAGTTTTTTAAAG
Cy5-PrQ-Tte	CUGGGUCGCAGUAACCCCAGUUAACAAAACAAGCCTT[Cy5]
IBRQ-ANTI-PrQTte	[IBRQ]TGGCTTGTTTTAT
ANTI-Tte-GGT-1	TGGCTTGTTTTATGA
ANTI-Tte-GGT-2	TGGCTTGTTTTATG
ANTI-Tte-GGT-3	TGGCTTGTTTTAT
ANTI-Tte-GGT-4	TGGCTTGTTTTA
ANTI-Tte-GGT-5	TGGCTTGTTTT
ANTI-Tte-GTT-1	TTGCTTGTTTTATGA
ANTI-Tte-GTT-2	TTGCTTGTTTTATG
ANTI-Tte-GTT-3	TTGCTTGTTTTAT
ANTI-Tte-GTT-4	TTGCTTGTTTTA
ANTI-Tte-GTT-5	TTGCTTGTTTT
Cy5-PrQ-Bsu	AGAGGUUCUAGCUACACCCUCUAUAAAAAACUAACCTT[Cy5]

IBRQ-ANTI-PrQBsu	[IBRQ]TGGTTAGTTTTTTA
ANTI-Bsu-GGT-1	TGGTTAGTTTTTTA
ANTI-Bsu-GGT-2	TGGTTAGTTTTTT
ANTI-Bsu-GGT-3	TGGTTAGTTTTT
ANTI-Bsu-GT-1	TGTTAGTTTTTTA
ANTI-Bsu-GT-2	TGTTAGTTTTTT
ANTI-Bsu-GT-3	TGTTAGTTTTT
Cy5-PrQ-Efa	ACUGGUUCGGAAACUUCCCAGAAUAAAAAACUAAGCCTT[Cy5]
IBRQ-ANTI-PrQEfa	[IBRQ]TGGCTTAGTTTTT
ANTI-Efa-GGT-1	TGGCTTAGTTTTT
ANTI-Efa-GGT-2	TGGCTTAGTTTT
ANTI-Efa-GGT-3	TGGCTTAGTTT
ANTI-Efa-GT-1	TGCTTAGTTTTT
ANTI-Efa-GT-2	TGCTTAGTTTT
ANTI-Efa-GT-3	TGCTTAGTTT

Table S2.2. Sequences of the **Translation prevention assay**. The T7 polymerase promotor is indicated in green. $PreQ_1$ riboswitch sequences indicated in orange. The essential cytosine (WT) or thymine (mutant) are underlined.

Name	**Sequence (5′ → 3′)**
Tte-WT fwd	TTAATACGACTCACTATAGGAATAACTGGGTCGCAGTAACCCCAGTAAAAAAACAAGG TACAATATGGTTTCAGGATGGC
Tte-Mutant fwd	TTAATACGACTCACTATAGGAATAACTGGGTCGCAGTAATCCCAGTAAAAAAACAAGG TACAATATGGTTTCAGGATGGC
Tte-rev	ATCAGCTAATTTTTTTAAATAAGCGCCATCCTGAAACCAT
Eco-WT fwd	TTAATACGACTCACTATAGGAATAATTGGGTTCCCTCACCCCAATCATAAAAAGGTAC AATATGGTTTCAGGATGGC
Eco-Mutant fwd	TTAATACGACTCACTATAGGAATAATTGGGTTCCCTCATCCCAATCATAAAAAGGTAC AATATGGTTTCAGGATGGC
Eco-rev	ATCAGCTAATTTTTTTAAATAAGCGCCATCCTGAAACCAT

Table S2.3. Sequences of the **Frameshifting assay**. $PreQ_1$ riboswitch sequences indicated in orange.

Name	**Sequence (5′ → 3′)**
T7sm-g	GGTAATACGACTCACTATAGGGAATTCTAGAAAGGAGATACCACCATG
pucrev3	CACGTTGTAAAACGACGGCCAGT
FS *Fnu* insert	CTAGTGACGCGGTGCTGGCAAAACCCGCGTAAAAAAACCAG
FS *Bsu* insert	CTAGTGCGCGGTTCTAGCTACACCCGCGTAAAAAAACTAAG
FS *Tte* insert	CTAGTGCGCGGTCGCAGTAACCCGCGTAAAAAAACAAG
FS *Eco* insert	CTAGTGCGCGGTTCCCTCACCCGCGTAAAAAAAAGGTT

Sequence entire PCR product with *Fnu* insert (5′ → 3′)

GGTAATACGACTCACTATAGGGAATTCTAGAAAGGAGATACCACCATGGCAGTGACCGGCTACCGG
CTGTTCGAGGAGATTCTGGCGGCCGCTGGTGGCGGGAGCGGAGGTGGAGGGTCGTCAGGTACCTTT
TTAAACTAGTGACGCGGTGCTGGCAAAACCCGCGTAAAAAAACCAGACAGCTTATCGCCATGGTCT
TCACACTCGAAGATTTCGTTGGGGACTGGGAACAGACAGCCGCCTACAACCTGGACCAAGTCCTTG
AACAGGGAGGTGTGTCCAGTTTGCTGCAGAATCTCGCCGTGTCCGTAACTCCGATCCAAAGGATTG
TCCGGAGCGGTGAAAATGCCCTGAAGATCGACATCCATGTCATCATCCCGTATGAAGGTCTGAGCG
CCGACCAAATGGCCCAGATCGAAGAGGTGTTTAAGGTGGTGTACCCTGTGGATGATCATCACTTTA
AGGTGATCCTGCCCTATGGCACACTGGTAATCGACGGGGTTACGCCGAACATGCTGAACTATTTCG
GACGGCCGTATGAAGGCATCGCCGTGTTCGACGGCAAAAAGATCACTGTAACAGGGACCCTGTGGA
ACGGCAACAAAATTATCGACGAGCGCCTGATCACCCCCGACGGCTCCATGCTGTTCCGAGTAACCA
TCAACAGCAGATCTAGCGGTGGTGGCGGGAGCGGCGGTGGAGGGTCATCGGGTTGTACAGAGATTG
CAGCGCTGGAGAAGGAGATCGCTGCGCTGGAGAAGGAGATTGCAGCGTTGGAGAAGGAGATCGCGG
CACTGGAGAAGGGCTAGCGGGCCCGAGTACCGAGCTCGAATTCACTGGCCGTCGTTTTACAACGTG

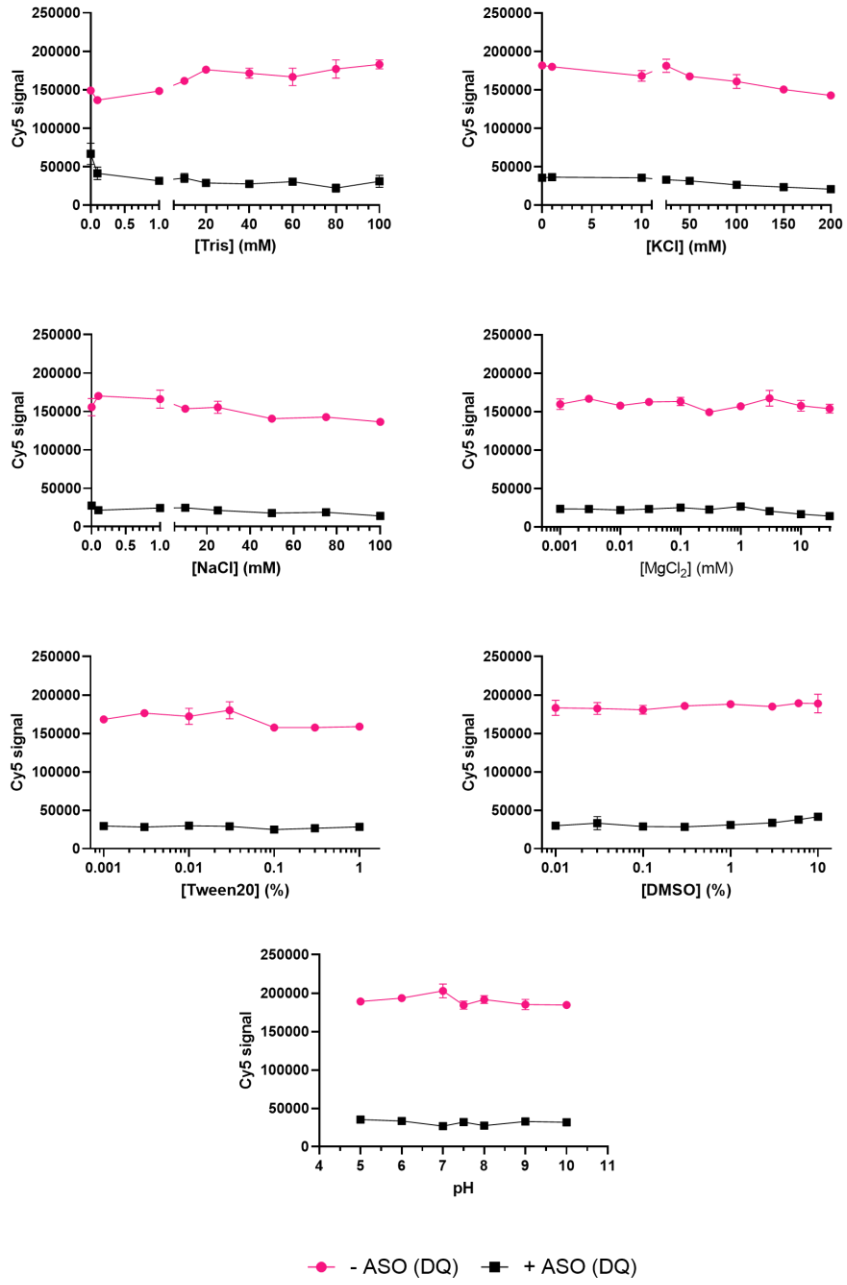

Figure S2.1. Buffer optimisation for the competitive binding antisense assay (CB ASsay) for the *Fusobacterium nucleatum* (*Fnu*) wildtype* (WT*) $PreQ_1$-I riboswitch. Standard buffer conditions were 100 mM Tris (pH = 7.5), 100 mM KCl, 10 mM NaCl, 1 mM $MgCl_2$, 0.1% (v/v) DMSO and 0.01% (v/v) Tween20, unless varied for optimisation.

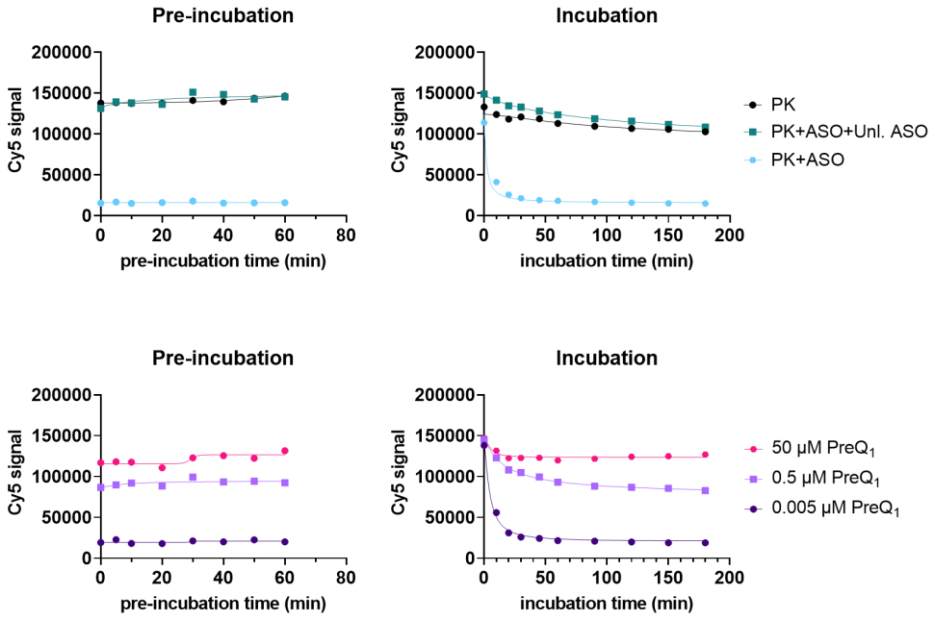

Figure S2.2. Incubation time optimisation for the competitive binding antisense assay (CB ASsay) for the *Fusobacterium nucleatum* (*Fnu*) wildtype* (WT*) $PreQ_1$-I riboswitch pseudoknot (PK). Standard incubation times were 1 hour pre-incubation of $PreQ_1$ riboswitch with ligand, and 2 hours incubation after labelled antisense oligonucleotide (ASO) addition, unless varied for optimisation.

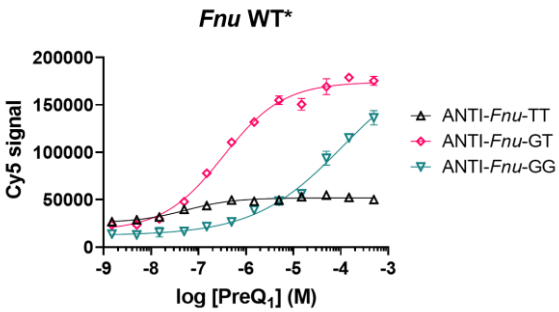

Figure S2.3. Competitive binding antisense assay (CB ASsay) of $PreQ_1$ with the *Fusobacterium nucleatum* (*Fnu*) wildtype* (WT*) $PreQ_1$-I riboswitch and three different antisense oligonucleotides (ANTI-*Fnu*-TT, -GT and -GG). All measurements were performed in duplicate.

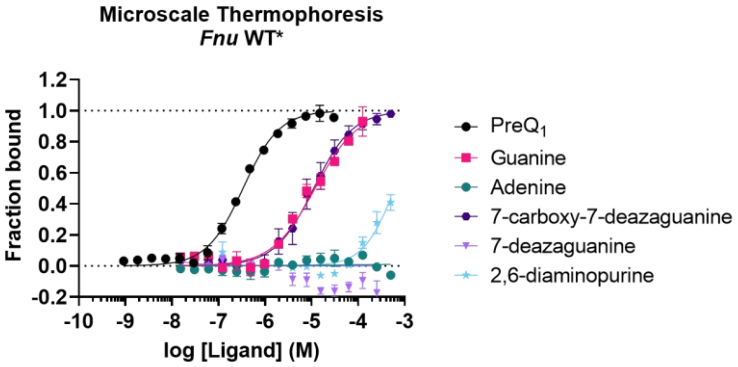

Figure S2.4. Microscale thermophoresis (MST) measurements of PreQ$_1$, guanine, adenine, 7-carboxy-7-deazaguanine, 7-deazaguanine and 2,6-diaminopurine to the *Fusobacterium nucleatum* (*Fnu*) wildtype* (WT*) PreQ$_1$-I riboswitch. Displayed datapoints represent the average of three separate measurements, from which mean and standard deviations were calculated with GraphPad Prism 8.

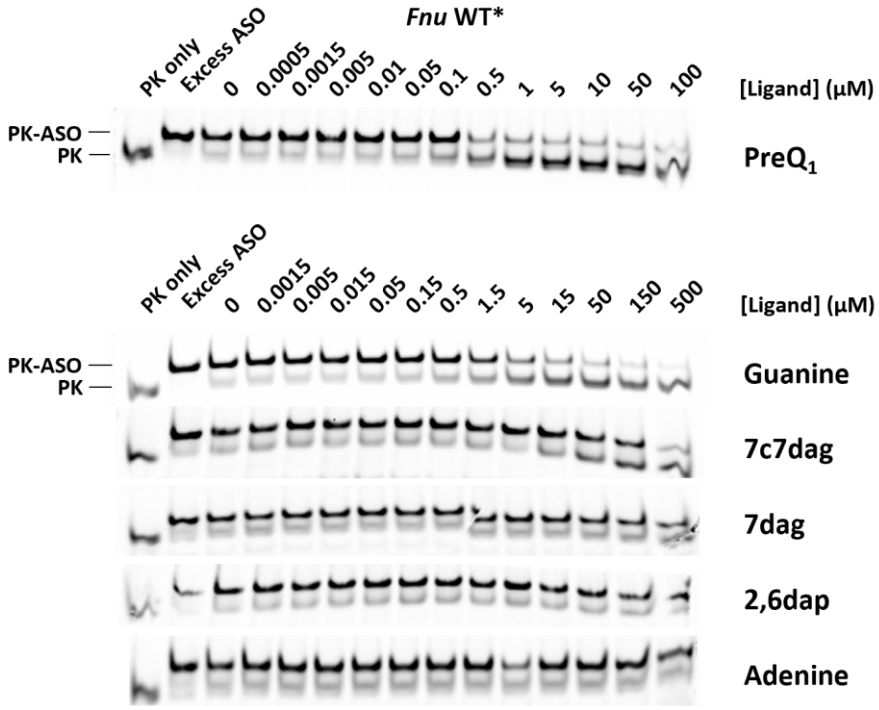

Figure S2.5. Competitive binding antisense assay (CB ASsay) with the *Fusobacterium nucleatum* (*Fnu*) wildtype* (WT*) PreQ$_1$-I riboswitch pseudoknot (PK) visualized on native PAGE. Cy5-PK (1 eq.) was pre-incubated with a ligand, after which unlabelled ASO (1 eq.) was added, and the two possible conformations (PK and PK-ASO) were separated on a 20% (w/v) polyacrylamide gel.

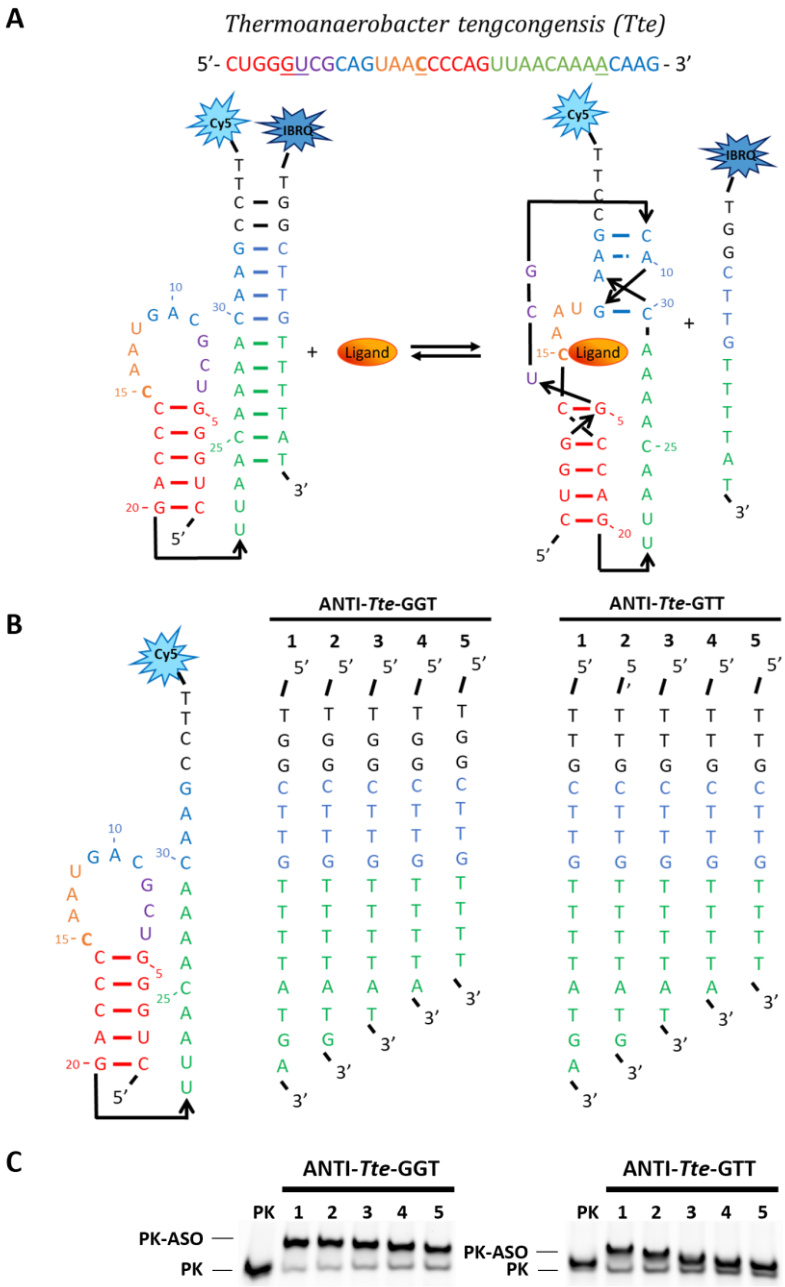

Figure S2.6. A) Schematic representation of the competitive binding antisense (CB ASsay) for *Thermoanaerobacter tengcongensis* (*Tte*) PreQ$_1$-I riboswitch. **B)** Antisense sequences for optimising the CB ASsay for the *Tte* riboswitch. **C)** CB ASsay of the *Tte* riboswitch with PreQ$_1$ and different antisense oligonucleotides (ASOs), visualized on a native PAGE. Cy5-PK (1 eq.) was incubated with unlabelled ASO (1 eq.) and the two possible conformations (PK and PK-ASO) were separated on a 20% (w/v) polyacrylamide gel.

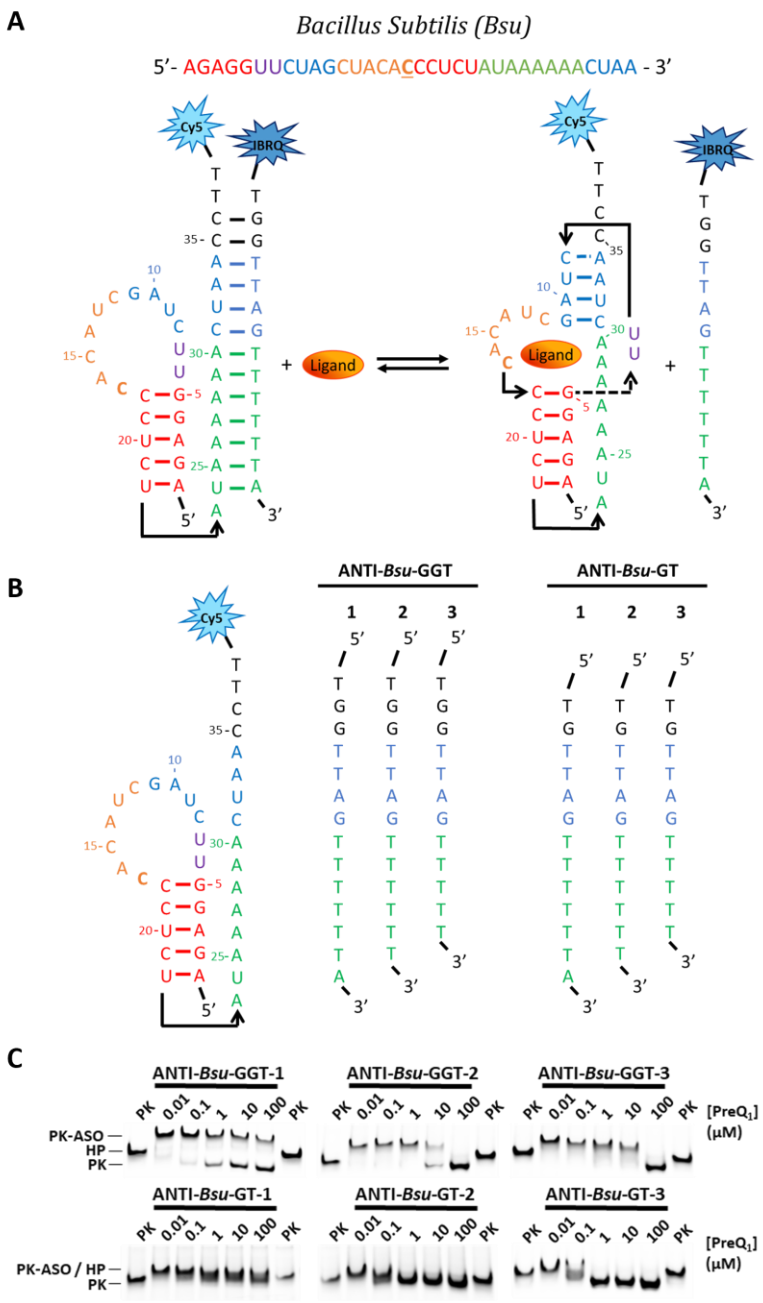

Figure S2.7. A) Schematic representation of the competitive binding antisense assay (CB ASsay) for the *Bacillus subtilis* (*Bsu*) $PreQ_1$-I riboswitch. **B)** Antisense sequences for optimising the CB ASsay for the *Bsu* riboswitch. **C)** CB ASsay of the *Bsu* riboswitch with $PreQ_1$ and different antisense oligonucleotides (ASOs), visualized on native PAGE. Cy5-PK (1 eq.) was pre-incubated with $PreQ_1$, after which unlabelled ASO (1 eq.) was added and the three possible conformations (hairpin (HP), pseudoknot (PK) and PK-ASO) were separated on a 20% (w/v) polyacrylamide gel.

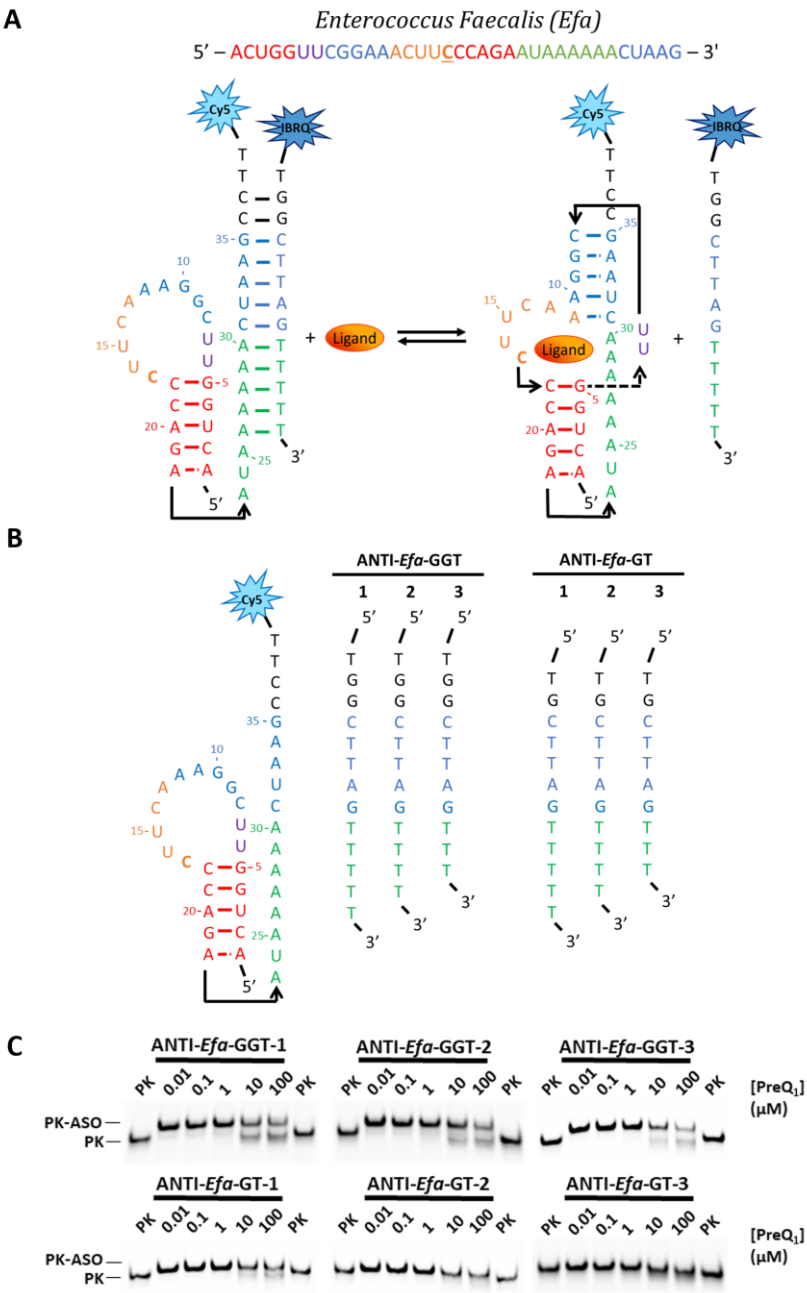

Figure S2.8. A) Schematic representation of the competitive binding antisense assay (CB ASsay) for the *Enterococcus faecalis* (*Efa*) $PreQ_1$-I riboswitch (ligand-bound conformation not experimentally proven). **B)** Antisense sequences for optimising the CB ASsay for the *Efa* riboswitch. **C)** CB ASsay of the *Efa* riboswitch with $PreQ_1$ and different antisense oligonucleotides (ASOs), visualized on native PAGE. Cy5-PK (1 eq.) was pre-incubated with $PreQ_1$, after which unlabelled ASO (1 eq.) was added, and the two possible conformations (PK and PK-ASO) were separated on a 20% (w/v) polyacrylamide gel.